

1  
2  
3  
4  
5  
6  
7  
8  
9  
10  
11  
12  
13  
14  
15  
16  
17  
18

## **Ribosome profiling reveals ribosome stalling on tryptophan codons upon oxidative stress in fission yeast**

Angela Rubio<sup>1</sup>, Sanjay Ghosh<sup>1,2</sup>, Michael Mülleder<sup>3</sup>, Markus Ralser<sup>3,4</sup>, Juan Mata<sup>1,5</sup>

1 Department of Biochemistry, University of Cambridge, UK

2 Current address: Institute of Bioinformatics and Applied Biotechnology, Bengaluru, India

3 The Molecular Biology of Metabolism Laboratory, The Francis Crick Institute, London, UK

4 Department of Biochemistry, Charité University Medicine, Berlin, Germany

5 Corresponding author

## 19 **ABSTRACT**

20 Modulation of translation is an essential response to stress conditions. We have investigated  
21 the translational programmes launched by the fission yeast *Schizosaccharomyces pombe*  
22 subject to five environmental stresses: oxidative stress, heavy metal, heat shock, osmotic  
23 shock and DNA damage. We also explored the contribution of two major defence pathways  
24 to these programmes: The Integrated Stress Response, which directly regulates translation  
25 initiation, and the stress-response MAPK pathway. To obtain a genome-wide and high-  
26 resolution view of this phenomenon, we performed ribosome profiling of control cells and of  
27 cells subject to each of the five stresses mentioned above, both in wild type background and  
28 in cells in which the Integrated Stress Response or the MAPK pathway were inactivated.

29 Translational changes were partially dependent on the integrity of both signalling pathways.  
30 Interestingly, we found that the transcription factor Fil1, a functional homologue of the Gcn4  
31 and Atf4 proteins (from budding yeast and mammals, respectively), was highly upregulated in  
32 most stresses. Consistent with this result, Fil1 was required for the normal response to most  
33 stresses. A large group of mRNAs were translationally downregulated, including many  
34 required for ribosome biogenesis. Overall, our data suggest that severe stresses lead to the  
35 implementation of a universal translational response, which includes energy-saving measures  
36 (reduction of ribosome production) and induction of a Fil1-mediated transcriptional  
37 programme.

38 Surprisingly, ribosomes stalled on tryptophan codons specifically upon oxidative stress, a  
39 phenomenon that is likely caused by a decrease in charged tRNA-Tryptophan. Tryptophan  
40 stalling led to a mild translation elongation reduction and contributed to the inhibition of  
41 initiation by the Integrated Stress Response. Taken together, our results show that different  
42 stresses elicit common and specific translational responses, revealing a special and so far  
43 unknown role in Tryptophan-tRNA availability.

44

## 45 INTRODUCTION

46 Cells react to stress situations such as starvation, changes in temperature, or the presence  
47 of toxic substances in their environment, by transcriptome and translation remodelling, as well  
48 as by the reconfiguration of their metabolism. Translation is the most energy-consuming  
49 process of the cell. Therefore, translational control plays an essential role by determining the  
50 rate of protein synthesis, which helps shape the composition of the proteome. Compared to  
51 transcriptional regulation, translational control of existing mRNAs allows for more rapid  
52 changes in protein levels, making this process particularly important upon stress exposure [1].  
53 In addition, as protein synthesis requires a large proportion of the cell energy, its regulation is  
54 related to the metabolic status of the cell [2]. Therefore, a tight control of translation is  
55 essential to cope with stress situations, and misregulation of this process often leads to  
56 disease [3].

57 In eukaryotes, translational control is often performed at the initiation stage [4], when the  
58 AUG start codon is identified and decoded by the initiator tRNA (Met-tRNA<sup>i</sup> Met). A key  
59 regulator of this process is the translation initiation factor eIF2, which is part of the so-called  
60 ternary complex (TC) together with the initiator tRNA and GTP. The TC, in complex with other  
61 translation initiation factors, binds to the 40S ribosomal subunit to form the 43S preinitiation  
62 complex (PIC). The 43S PIC is recruited to the 5' cap of the mRNA by additional initiation  
63 factors, leading to the formation of the 48S PIC, which scans the mRNA until the initiation  
64 codon is reached. At this step, the 60S subunit binds the complex and GTP is hydrolysed.  
65 eIF2-GDP must then be recycled to eIF2-GTP by the GTP/GDP-exchange factor eIF2B. After  
66 stress exposure, the eIF2 $\alpha$  subunit is phosphorylated at a specific serine residue (serine 51 in  
67 mammals and 52 in fission yeast), and binds to eIF2B acting as a competitive inhibitor, which  
68 reduces levels of the ternary complex and triggers a global down-regulation of translation [5,6].

69 The pathway that regulates translation through eIF2 $\alpha$  phosphorylation is called the  
70 Integrated Stress Response. In mammals, there are four eIF2 $\alpha$  kinases (Hri, Gcn2, Pek/Perk  
71 and Pkr) that are activated by different stresses and inhibit translation initiation through the  
72 phosphorylation of eIF2 $\alpha$  [4]. In the yeast *Saccharomyces cerevisiae*, Gcn2 is the sole eIF2 $\alpha$   
73 kinase [7,8]. In the fission yeast *Schizosaccharomyces pombe*, three eIF2 $\alpha$  kinases (Gcn2,  
74 Hri1 and Hri2) show distinct and overlapping activation patterns in response to cellular  
75 stresses [9,10]. Whereas Hri2 is mainly activated in response to heat shock and Hri1 at  
76 stationary phase in response to nutritional limitation, Gcn2 is the main eIF2 $\alpha$  kinase activated  
77 in early exposure to H<sub>2</sub>O<sub>2</sub> and MMS [9–11].

78 In parallel to the general downregulation of translation upon stress, there is an induction of  
79 the translation of specific mRNAs, some of them encoding transcription factors, which in turn  
80 promote the transcriptional response. Recently, we have shown that amino acid starvation in

81 *S. pombe* increases the translation of the transcription factor Fil1, the functional orthologue of  
82 Atf4 in mammals and Gcn4 in budding yeast, through the activation of the Gcn2-eIF2 $\alpha$   
83 pathway [12]. Fil1 is required for the transcriptional response to amino acid starvation as well  
84 as for normal growth in minimal medium lacking amino acids. Furthermore, Fil1 is regulated  
85 in a similar manner through inhibitory upstream ORFs (uORFs) located at the 5'-leader  
86 sequence (six uORFs in *fil1*, four in *GCN4* and two in *ATF4*) [12]. In budding yeast and  
87 mammalian cells, eIF2 $\alpha$  phosphorylation reduces the abundance of active ternary complexes  
88 and the reinitiation of translation occurs after bypassing the inhibitory uORFs, which allows  
89 the scanning subunit to reach the main coding sequence [8,13]. Notably, Fil1 does not show  
90 sequence similarity to either Gcn4 or Atf4 [12].

91 Gene expression programs in response to stress are also regulated by Stress Activated  
92 Protein Kinases (SAPK). A key player in this pathway in *S. pombe* is the mitogen-activated  
93 protein kinase (MAPK) Sty1/Spc1 [14,15], which is homologous to the Hog1 osmo-sensing  
94 MAPK in *S. cerevisiae* and to the mammalian and *Drosophila* JNK and p38 SAPKs [16].

95 Stress signals activate and phosphorylate Sty1, promoting its transient accumulation in the  
96 nucleus, where it triggers a wide transcriptional shift of the gene expression program. This  
97 transcriptional response is mediated by the Atf1 transcription factor [17–20]. Sty1 also has a  
98 role in the translational response to stress. First, cells show higher levels of eIF2 $\alpha$   
99 phosphorylation in the absence of Sty1 [10,21]. Second, Sty1 associates *in vivo* with the  
100 translation elongation factor 2 (eEF2) and the translation initiation factor 3a (eIF3a) [22].  
101 Finally, the presence of Sty1 is required to maintain the levels and the phosphorylation of  
102 eIF3a, and the recovery of translation levels after stress is less efficient in the absence of Sty1  
103 [21,22].

104 Translation upon stress can be also regulated at the elongation step through the abundance,  
105 modification, and charging levels of transfer RNA (tRNA) [23]. tRNA is the most extensively  
106 modified RNA and many post-transcriptional nucleoside modifications occur at the anticodon  
107 loop [24]. These modifications can change the stability or localization of tRNAs [25], as well  
108 as the fidelity and efficiency of translation [26]. It has also been shown that tRNA  
109 fragmentation occurs upon stress in eukaryotes [27] and, in human cells, that tRNA fragments  
110 have a role in translation repression [28].

111 Ribosome profiling (ribo-seq) provides a genome-wide and high-resolution view of  
112 translational control. The approach is based on the treatment of translating ribosome–mRNA  
113 complexes with a ribonuclease (RNase), in such a way that only RNA fragments protected by  
114 bound ribosome survive the treatment. These fragments are then isolated and analysed by  
115 high-throughput sequencing. The number of sequence reads that map to a coding sequence,  
116 normalized by mRNA levels, provides an estimate of the efficiency of translation for every  
117 cellular mRNA [29]. In addition, the position of the reads on the genome identifies the location

118 of ribosomes on the mRNA. This information can be used to determine relative ribosome  
119 occupancies on each codon, which allow the detection of ribosomes stalled on specific codons  
120 [12,30,31].

121 Although some stress-induced gene expression programs have been studied in detail at the  
122 genome-wide level [14,15,32–36], the effects of different stresses have been examined in  
123 isolation, making comparisons across stresses difficult. Moreover, to our knowledge, there  
124 are no systematic studies of the role of major stress-response pathways on genome-wide  
125 translation programmes. Here we use *S. pombe* to investigate similarities and differences  
126 among the translational responses to five commonly studied stress situations: exposure to  
127 H<sub>2</sub>O<sub>2</sub> (oxidative stress), cadmium (heavy metal), and methyl methanesulfonate (MMS,  
128 genotoxic stress), sorbitol treatment to induce osmotic shock, and heat shock. We perform  
129 ribosome profiling in control and stressed cells, under highly controlled and comparable  
130 conditions. We also investigate the contribution of the Integrated Stress Response (mediated  
131 by eIF2 $\alpha$  phosphorylation) and the stress-responsive MAPK pathway (Sty1) to these  
132 translation programs. Overall, we found that translation is typically downregulated, but  
133 activated for very few genes. Interestingly, the Fil1 transcription factor is strongly induced at  
134 the translational level upon several stresses, in a manner strongly dependent on eIF2 $\alpha$   
135 phosphorylation. Moreover, Fil1 is required for the full implementation of stress-responsive  
136 transcription programs. These stresses also cause a rapid translational downregulation of  
137 genes involved in ribosome biogenesis and ribosomal proteins.

138 Surprisingly, we found that ribosomes stall selectively on tryptophan codons upon oxidative  
139 stress, a phenomenon that is likely to be caused by a decrease in the levels of charged tRNA-  
140 Tryptophan (tRNA-Trp). This specific stalling on tryptophan led to a mild elongation defect.  
141 Our results suggest that different stresses elicit common and specific translational responses,  
142 both at the initiation and the elongation levels, and uncovers a novel and specific role to  
143 tryptophan tRNA availability.

144

## 145 **RESULTS**

### 146 **Transcriptomic responses to stress**

147 To investigate genome-wide effects of stress on gene expression, we carried out two  
148 independent ribosome profiling experiments (with parallel RNA-seq) of *S. pombe* cells subject  
149 to five different stress-inducing treatments for 15 minutes: 0.5 mM H<sub>2</sub>O<sub>2</sub> (oxidative stress), 0.5  
150 mM CdSO<sub>4</sub> (heavy metal exposure), temperature shift from 32°C to 39°C (heat shock), 1 M  
151 sorbitol (osmotic shock) and 0.02% methyl methanesulfonate (MMS, an alkylating agent that  
152 causes DNA damage). To study the contribution of the eIF2 $\alpha$  phosphorylation and Sty1  
153 pathways we performed parallel experiments with the mutant strain *eIF2 $\alpha$ -S52A*, which  
154 expresses a non-phosphorylatable version of eIF2 $\alpha$ , and a *sty1 $\Delta$*  strain, in which the main

155 stress-responsive MAPK pathway is inactive. These conditions have been used in the past  
156 for microarray-based transcriptomics, and have been shown to elicit robust transcriptional  
157 responses within a similar timeframe while maintaining high cell viability [14]. All experiments  
158 were carried out using rich medium (YE), as *sty1Δ* cells grow very poorly in minimal medium.

159 We first examined the transcriptional responses to stress using the RNA-seq data. As we  
160 did not perform a global correction for total mRNA abundance, the discussion below refers to  
161 relative changes in gene expression. There were more genes significantly up-regulated than  
162 down-regulated in every strain and condition (Table 1). For the specific stress conditions that  
163 we employed (e.g. concentration of stressor and time), the changes were stronger after heat  
164 and cadmium stress, but genes induced by the five stress treatments overlapped significantly  
165 with one another. A similar overlap across stresses was observed for repressed genes  
166 (highest P value  $< 2 \times 10^{-5}$  in wild type cells). Figure S1A shows a heat map with over 1,200  
167 genes that are differentially expressed in at least one condition in wild-type cells. Most of the  
168 regulated genes behave similarly in wild type and *eIF2α-S52A* cells. By contrast, the  
169 transcriptional response to stress in *sty1Δ* cells was substantially weaker although not  
170 completely abolished [14] (Fig. S1A). Consistently, the numbers of induced and repressed  
171 genes were comparable among wild type and the *eIF2α-S52A* mutant but were lower in *sty1Δ*  
172 cells (Table 1).

173 The Core Environmental Stress Response (CESR) was defined in a microarray study as  
174 those genes induced or repressed two-fold or greater in most of the five stresses analysed  
175 [14]. Consistent with the microarray data, the majority of induced and repressed CESR genes,  
176 as well as stress-specific genes, were also differentially expressed in our RNA-seq  
177 experiments (Fig. 1A, B and Fig. S1B, S1C). Overall, our data show that transcriptomic  
178 responses to stress are largely independent of eIF2α phosphorylation, but strongly reliant on  
179 the MAPK pathway.

180

### 181 **General translational responses to stress**

182 Activation of the Integrated Stress Response by stress leads to general translational down-  
183 regulation, mediated through eIF2α phosphorylation. To investigate the level of activation of  
184 this pathway and its effect on global translation levels, we monitored eIF2α phosphorylation  
185 levels by immunoblotting and analysis of polysome profiles on sucrose gradients. For the  
186 specific conditions we used (single stressor concentration and 15-minute exposures),  
187 cadmium, heat shock and H<sub>2</sub>O<sub>2</sub> treatments led to increased eIF2α phosphorylation levels (Fig.  
188 1C) and lower polysomes to subpolysomes ratios (Fig. 1D-G), the latter being indicative of a  
189 decrease in translation initiation. Both effects were also detected, although less pronounced,  
190 after the MMS and sorbitol treatments (Fig. 1C, 1G). *eIF2α-S52A* cells reduced the polysomes  
191 to subpolysomes ratio in response to stress, albeit to a lesser extent than wild-type cells (Fig.

192 1D-G). This partial dependency on eIF2 $\alpha$  phosphorylation is in agreement with recent  
 193 reports of *S. pombe* responses to UV and oxidative stress [35,37,38]. By contrast, the Sty1  
 194 protein was not required for the downregulation of translation initiation (Fig. 1F, G). Indeed,  
 195 in some cases (H<sub>2</sub>O<sub>2</sub> and sorbitol), *sty1* $\Delta$  cells reduced translation more than wild type cells  
 196 (Fig. 1G). Thus, since polysome profiling cannot distinguish between unaltered active  
 197 translation and slowed-down elongation, our polysome profiling data suggest that translation  
 198 is affected at least at the initiation step upon cadmium, heat shock and H<sub>2</sub>O<sub>2</sub> exposure. This  
 199 effect is only partially dependent on eIF2 $\alpha$  phosphorylation. In addition, the Sty1 MAPK  
 200 pathway may also modulate translation initiation under some stresses [10,21].

201

### 202 Gene-specific translational regulation upon stress exposure

203 We used ribosome profiling to investigate gene-specific translational control in response to  
 204 stress. Ribosome-protected fragments (RPFs) were isolated and analysed by high-throughput  
 205 sequencing, whereas mRNA levels were estimated in parallel by RNA-seq. The number of  
 206 RPFs mapped to each coding gene, normalized by the corresponding number of RNA-seq  
 207 reads, was used to calculate relative translation efficiencies (TEs) (Fig. 2A). Genes showing  
 208 significant changes in TE upon stress treatment were identified using RiboDiff (see Methods),  
 209 with thresholds of a minimum 1.5-fold change and adjusted P value < 0.01. This approach  
 210 does not consider global changes in gene expression and, therefore, may overestimate TE  
 211 values. Nevertheless, these TE values reflect relative changes among conditions and among  
 212 genetic backgrounds, and identifies genes that behave differently from the majority of  
 213 transcripts.

214

215 **Table 1. Number of transcripts regulated after stress exposure on each strain.**

	mRNA up			mRNA down			Translation up			Translation down		
	<i>wt</i>	<i>S52A</i>	<i>sty1</i> $\Delta$	<i>wt</i>	<i>S52A</i>	<i>sty1</i> $\Delta$	<i>wt</i>	<i>S52A</i>	<i>sty1</i> $\Delta$	<i>wt</i>	<i>S52A</i>	<i>sty1</i> $\Delta$
<b>CdSO<sub>4</sub></b>	443	410	176	302	269	111	57	37	17	320	212	103
<b>HS</b>	621	468	306	404	364	149	39	18	1	229	124	5
<b>H<sub>2</sub>O<sub>2</sub></b>	186	120	25	36	50	18	7	1	3	49	0	65
<b>MMS</b>	142	147	0	8	22	0	4	2	0	1	0	0
<b>Sorbitol</b>	193	198	0	113	109	0	0	0	0	1	1	7

216

217 Numbers of mRNAs regulated during five stress conditions in three genetic backgrounds: wild  
 218 type, *eIF2 $\alpha$ -S52A* and *sty1* $\Delta$  cells. mRNA up/down, and translation up/down indicate numbers  
 219 of mRNAs whose expression is significantly up- or down-regulated at the transcriptome or

220 translational levels, respectively (see Methods for details). Annotated lists containing these  
221 genes are presented in Datasets S1/ S2.

222

223

224 Upon stress, the number of translationally regulated genes was much smaller than those  
225 affected at the transcript level (Table 1). In relative terms, unlike transcriptomic responses,  
226 the numbers of translationally down-regulated genes were higher than those up-regulated  
227 (Table 1). Thus, the gene-specific translational response seems to be targeted to reduce  
228 mRNA translation. The treatment that had the strongest effect was cadmium, followed by heat  
229 shock and H<sub>2</sub>O<sub>2</sub>, while fewer changes were detected upon the applied MMS and sorbitol  
230 concentrations (Table 1). This trend is generally similar to transcriptional and eIF2 $\alpha$   
231 phosphorylation changes (Fig. 1), indicating that gene expression programs in response to  
232 the latter stresses are generally weaker.

233 We found 82 translationally upregulated genes in wild type cells in at least one stress  
234 treatment, 28 of which overlapped with the CESR induced genes (P value < 5x 10<sup>-15</sup>). Of  
235 those 82 genes, four were induced in all the stress conditions except for sorbitol, and 15 were  
236 shared across cadmium and heat shock. We could not find any specific GO category enriched  
237 within the 82 genes (see Methods). Yet, the data included individual genes that have  
238 previously linked to the stress response. An example of cadmium-upregulated gene (both  
239 transcriptionally and translationally) was *prf1*, which encodes a transcription factor involved in  
240 the oxidative stress response and sexual differentiation [39–41] (Fig. S2A). This regulation is  
241 consistent with the generation of reactive oxygen species after cadmium stress [42]. Other  
242 interesting genes were related to protein catabolism (*ubp3*, in cadmium and heat shock),  
243 autophagy (*atg3*, in cadmium), cell cycle (*srk1*, in cadmium), DNA repair (*dna2*, in heat shock  
244 and *uve1*, in H<sub>2</sub>O<sub>2</sub> and cadmium), transmembrane transport, carbohydrate and amino acid  
245 metabolism. The most translationally upregulated gene was *fil1* [12], which encodes a  
246 transcription factor essential for the response to amino acid starvation (Fig. 2A). The role of  
247 this gene in stress responses is discussed in detail below. Finally, we found that upon  
248 cadmium and heat shock treatments, more than 45% of translationally upregulated genes  
249 were also transcriptionally induced, whereas less than 14% of translationally downregulated  
250 were also transcriptionally repressed. This coordination of transcriptomic and translational  
251 induction (potentiation) has been observed by polysome profiling in budding and fission yeast  
252 responses to stress [36,43].

253 We also identified 382 translationally down-regulated genes (translation efficiency repressed  
254 in at least one condition), 149 of which were part of the CESR-repressed list (P value < 5x 10<sup>-73</sup>).  
255 Like the induced genes, cadmium, heat shock and H<sub>2</sub>O<sub>2</sub> led to stronger effects, whereas  
256 the consequences of MMS and sorbitol exposure were very mild (Table 1). The most



257 extensive overlap was between cadmium and heat shock stress, with 170 genes shared.  
258 These genes included *cdr2*, which is involved in the regulation of the G2/M transition through  
259 the inhibition of the Wee1 kinase [44] (Fig. S2B). Repression of this gene is consistent with  
260 the block of cell cycle progression in response to stress. There was also a substantial overlap  
261 (38 genes) among cadmium, heat shock and H<sub>2</sub>O<sub>2</sub> stresses. These data indicate that heavy  
262 metal exposure, oxidative conditions and heat shock are strong stresses under the conditions  
263 used in this work, and that they cause similar translational responses.

264 Translationally repressed genes were mainly associated with cytoplasmic translation  
265 (GO:0002181; P = 10<sup>-89</sup>), ribosome biogenesis (GO:0042254; P = 10<sup>-28</sup>) and ribosome  
266 assembly (GO:0042255; P = 10<sup>-11</sup>). Consistently, 110 of the 382 down-regulated genes  
267 encoded ribosomal proteins. (Fig. 2A, B). We have previously observed this effect upon  
268 nitrogen depletion [30] and amino acid starvation [12], demonstrating that this is a widespread  
269 translational response to stress.

270 Finally, we investigated whether translational responses were dependent on the major stress  
271 response pathways. Many TE-upregulated genes were partially induced in both *eIF2α-S52A*  
272 and *sty1Δ* mutants (Fig. 2C). However, a direct comparison of the induction levels in wild type  
273 and mutant cells (Fig. 2E), revealed that the upregulation in the mutant was impaired for most  
274 genes. A very similar dependency was observed for downregulated genes (Fig. 2D, F), which  
275 were generally less repressed in both mutant backgrounds. Therefore, both the eIF2α and the  
276 MAPK pathways contribute to a normal translational response, but neither of them is sufficient  
277 to explain the response in its entirety.

278

### 279 ***Fil1* is the major translational responder to stress**

280 The transcription factor *fil1* was induced very strongly at the translation efficiency level by  
281 cadmium, heat shock, and H<sub>2</sub>O<sub>2</sub> treatments, while showing small reductions or no changes in  
282 mRNA levels (Fig. 3A, B). There was also a weak translational induction after MMS treatment,  
283 but none after the sorbitol doses applied. These data mirror the change in eIF2α  
284 phosphorylation in these stresses (Fig. 1C). Consistently, the translational induction of *fil1*  
285 was completely dependent on eIF2α phosphorylation, and very weakly on Sty1 signalling (Fig.  
286 3A). We investigated if this increase in TE was accompanied by higher protein levels. To do  
287 this, cells expressing Fil1-TAP from their endogenous locus were used to compare protein  
288 levels by immunoblot in the five stress conditions. Consistent with the TE data, there was a  
289 strong increase in protein levels after cadmium, heat shock and H<sub>2</sub>O<sub>2</sub> treatments, weaker after  
290 MMS, and none upon sorbitol (Fig. 3C, D and Fig. S2 C-E). The kinetics of the *fil1* induction  
291 was stress-specific, with cadmium and heat shock showing a transient response (peaking at  
292 15 minutes) and H<sub>2</sub>O<sub>2</sub> and MMS showing slower responses. In particular, the increase at 60  
293 minutes after H<sub>2</sub>O<sub>2</sub> and MMS (Fig. 3D and Fig. S2D) was analogous to the behaviour of CESR-

294 induced genes under the same conditions, whose induction persisted for an hour [14]. The  
295 variety in induction kinetics suggests that Fil1 protein induction may be regulated at other  
296 levels in addition to translation. Consistent with the ribosome profiling data, no Fil1 protein  
297 induction was detected in *eIF2 $\alpha$ -S52A* cells (Fig. 3C, D and Fig. S2C-E). Surprisingly, Fil1  
298 protein levels were higher in *sty1 $\Delta$*  than in wild type cells, even in the absence of stress (Fig.  
299 3C, D and Fig. S2C-E). This may relate to the fact that *sty1 $\Delta$*  cells are sensitive to stress [45–  
300 48]. Indeed cells lacking this protein show evidence of an induced stress response even under  
301 normal laboratory growth conditions [14]. Taken together, these data indicate that *fil1*  
302 translational induction upon stress leads to an increase in Fil1 protein levels in an eIF2 $\alpha$ -  
303 dependent manner, and that the Sty1 MAPK pathway modulates this effect. This response  
304 takes place in rich medium, where Fil1 is not required for normal growth [12]. Therefore, Fil1  
305 behaves as a general stress-responsive transcription factor.

306 We then investigated the role of Fil1 in the transcriptional responses to stress. We performed  
307 RNA-seq experiments in the five stress conditions in cells lacking *fil1*, and monitored the  
308 behaviour of 165 previously identified Fil1 targets [12]. Note that Fil1 targets were defined as  
309 genes that showed lower expression in *fil1 $\Delta$*  cells in minimal medium and in the absence of  
310 stress [12]. In unstressed cells growing in rich medium, Fil1 targets were expressed at slightly  
311 lower levels in the *fil1 $\Delta$*  mutant (Fig. 4A-C and Fig. S3A, B). In response to cadmium, heat  
312 shock and H<sub>2</sub>O<sub>2</sub> treatments, Fil1 targets were expressed at substantially decreased levels in  
313 the mutant (Fig. 4A-C and Fig. S3A, B). Consistently, Fil1 target genes overlapped  
314 significantly with genes underexpressed in *fil1 $\Delta$*  cells at 15 minutes after heat shock (Fig. 4D),  
315 and with genes underexpressed 60 minutes after H<sub>2</sub>O<sub>2</sub> treatment (Fig. 4E). These data  
316 demonstrate that Fil1 promotes the expression of a common group of genes in response to  
317 strong stresses (cadmium, heat shock and H<sub>2</sub>O<sub>2</sub> treatments).

318 These results suggest that Fil1 may be important for survival to stress in rich medium. We  
319 explored this hypothesis by performing viability assays of wild type and *fil1 $\Delta$*  mutant under the  
320 five stress treatments. *fil1 $\Delta$*  cells were sensitive to high temperature, H<sub>2</sub>O<sub>2</sub> and MMS, whereas  
321 no difference to wild-type was observed at the sorbitol concentrations applied. Surprisingly,  
322 cells lacking Fil1 were resistant to cadmium treatment (Fig. 4F). Although the reason for this  
323 phenotype is unclear, deletion of genes encoding other transcription factors involved in stress  
324 response (*atf1*) [39,49], and of genes encoding several RNA-binding proteins [50] show similar  
325 resistance to cadmium.

326 As mentioned above, Fil1 is necessary for the normal expression of its targets in response  
327 to several stresses (Fig. 4A-C), and Fil1 expression was induced under the same conditions  
328 in an eIF2 $\alpha$ -dependent manner (Fig. 3 C, D and Fig. S2C). To investigate if *fil1* induction is  
329 required for the normal expression of Fil1 targets, we compared the expression levels of *fil1*  
330 targets upon stress in wild type and eIF2 $\alpha$ -S52A mutants. After 15 minutes of treatment, Fil1

331 target levels were mildly increased by heat shock and H<sub>2</sub>O<sub>2</sub> (but not by cadmium) in an eIF2 $\alpha$ -  
332 dependent manner (Fig. S3C). As Fil1 targets tend to be induced more strongly by H<sub>2</sub>O<sub>2</sub> at  
333 later time points (Fig. 4C), we repeated the experiment upon a 60-minute H<sub>2</sub>O<sub>2</sub> exposure.  
334 Indeed, this led to a late and stronger induction of Fil1 targets that was almost completely  
335 dependent on eIF2 $\alpha$  phosphorylation (Fig. S3D). These results indicate that, at least in some  
336 conditions, *fil1* translational upregulation plays a role in the implementation of the normal  
337 transcriptional responses to stress.

338 In addition, cells lacking Sty1 showed increased mRNA levels of Fil1 targets in both stressed  
339 and unstressed cells (Fig. S3E). Indeed, the overlap between upregulated genes in  
340 unstressed *sty1* $\Delta$  cells and Fil1-dependent genes was significant ( $P= 3.5 \times 10^{-11}$ ). These data  
341 are also consistent with the increased Fil1 protein levels in unstressed *sty1* $\Delta$  cells (Fig. 3C-D  
342 and Fig. S2C-E). These data suggest that the Sty1 MAPK pathway cross-talks with the  
343 Integrated Stress Response, consistent with previous observations [10,21].

344

### 345 **Ribosome occupancy on tryptophan codons is increased upon oxidative** 346 **stress**

347 Ribosome profiling provides information on ribosome locations with codon-level resolution  
348 and can thus be used to detect codon-specific ribosome stalling caused by stress conditions.  
349 To investigate this level of regulation, we quantified the fraction of ribosomes translating each  
350 of the 61 amino acid-encoding codons, normalized by the abundance of the corresponding  
351 codon in the transcriptome. This 'relative codon occupancy' reflects the average time spent  
352 by the ribosome on each codon. Strikingly, the single codon for tryptophan (TGG) showed  
353 strongly increased ribosome occupancy upon H<sub>2</sub>O<sub>2</sub> treatment (Fig. 5A, S4A). This enrichment  
354 was highly specific, as it was not observed for any other codon, and in any other stress  
355 condition (Fig. S4B).

356 A possible explanation for this observation was that cellular tryptophan levels decreased  
357 because of H<sub>2</sub>O<sub>2</sub> treatment. We therefore measured intracellular amino acid concentrations  
358 by mass spectrometry. We observed a reduction of approximately 20% in tryptophan levels.  
359 However, this change was borderline of statistical significance ( $P=0.04$ ), and was smaller  
360 than that of other amino acids that did not show any difference in ribosome occupancy of their  
361 cognate codons (Fig. 5F, S4C). In addition, mRNA levels and TE of the tRNA-Trp ligase,  
362 encoded by *wrs1* gene, remained unaffected.

363 A second hypothesis was that the levels of tRNA charging could be affected by oxidative  
364 stress. To investigate this possibility, we compared the levels of amino-acylated (charged)  
365 and deacylated (uncharged) tRNA-Trp. tRNAs were first subjected to periodate oxidation.  
366 This treatment leads to the removal of the 3' nucleotide of uncharged tRNAs through  $\beta$ -

367 elimination, whereas the charged fraction is protected by the amino acid and remains  
368 unaltered. The tRNAs are then deacylated at high pH. Thus, uncharged and charged tRNAs  
369 show a difference of one nucleotide in size, which can be detected by polyacrylamide gel  
370 electrophoresis and Northern blotting [51] (Fig. 5B). tRNA-Trp deacylated samples were used  
371 as controls and showed that total levels of tRNA-Trp were not affected by oxidative stress, as  
372 well as ruling out the fragmentation of tRNAs [27] (Fig. 5B). By contrast, tRNA-Trp charging  
373 levels were reduced more than two-fold after H<sub>2</sub>O<sub>2</sub> treatment (Fig. 5B, C). To confirm that this  
374 effect is specific of tRNA-Trp, we verified that charged tRNA-His levels remained identical  
375 upon H<sub>2</sub>O<sub>2</sub> treatment (Fig. 5D). The addition of supplemental tryptophan to rich medium two  
376 hours before, or only during the H<sub>2</sub>O<sub>2</sub> treatment, prevented the charged tRNA-Trp drop and  
377 increased the charging levels (Fig. 5E). Thus, these data indicate that the increase in  
378 ribosome occupancy at the tryptophan codon in H<sub>2</sub>O<sub>2</sub> stress condition reflects a reduced  
379 charged tRNA-Trp fraction.

380

### 381 **Decreased tRNA-Trp charging may affect eIF2 $\alpha$ phosphorylation**

382 In *S. cerevisiae* uncharged tRNAs activate the Gcn2 kinase, which phosphorylates eIF2 $\alpha$  to  
383 downregulate global translation initiation in response to amino acid starvation [7]. Recently, it  
384 has been shown that Gcn2 in *S. pombe* is activated in response to UV and oxidative stress  
385 through a mechanism that involves Gcn1 and most likely the binding of tRNAs [52]. Thus, we  
386 reasoned that increased levels of uncharged tRNA-Trp upon H<sub>2</sub>O<sub>2</sub> treatment might contribute  
387 to eIF2 $\alpha$  phosphorylation. To explore this possibility, we compared eIF2 $\alpha$  phosphorylation  
388 levels upon H<sub>2</sub>O<sub>2</sub> stress in the presence and absence of supplemental tryptophan in rich  
389 medium. Consistent with this idea, addition of tryptophan (which increases tRNA-Trp charging  
390 levels, see above) caused a reduction of eIF2 $\alpha$  phosphorylation (Fig. 6C). These data suggest  
391 that uncharged tRNA-Trp could promote Integrated Stress Response signalling upon H<sub>2</sub>O<sub>2</sub>  
392 exposure in rich medium, and thus affect both translation initiation and translation elongation.

393 Differences in charged tRNA-Trp levels cannot affect codon usage because tryptophan is  
394 encoded by only one codon, TGG. However, as tryptophan is the least frequent amino acid  
395 in proteins (less than 0.015% on average), we asked whether the translation efficiency of  
396 genes containing more tryptophan might be affected by lower charged tRNA-Trp levels upon  
397 H<sub>2</sub>O<sub>2</sub> stress. Genes were ranked by the percentage of tryptophan codons in their coding  
398 sequences, and assigned to 11 bins. We then measured the apparent change in translation  
399 efficiency upon oxidative stress for each bin. The data showed a trend towards increased  
400 translation efficiency changes after H<sub>2</sub>O<sub>2</sub> treatment with higher tryptophan content, which was  
401 not observed in other stresses (Fig. 6A and Fig. S5). We also ruled out that this trend was  
402 determined by transcript lengths (Fig. 6B). The group of genes lacking tryptophan is enriched  
403 in genes encoding ribosomal proteins ( $P = 10^{-27}$ ), which have a small transcript size (Fig. 6B).

404 By contrast, the group with the most tryptophan (0.023-0.056%) showed an enrichment in  
405 genes related to lipid biosynthesis (GO:0008610;  $P = 6.6 \times 10^{-10}$ ), protein glycosylation  
406 (GO:0006486;  $P = 4 \times 10^{-7}$ ) and cell wall biogenesis (GO:0071554;  $P = 1.5 \times 10^{-5}$ ). This  
407 enrichment is consistent with the fact that tryptophan is an amphipathic amino acid, often  
408 found in transmembrane domains. Given that translation efficiency as defined above is a  
409 relative measurement of the number of ribosomes per transcript (normalised to mRNA  
410 abundance), an increase in this parameter in tryptophan-rich genes is likely to reflect a  
411 slowdown of translation elongation of these genes rather than an increase in their protein  
412 synthesis. Thus, we propose that oxidative stress modulates translation at two levels: at  
413 initiation, through the Integrated Stress Response, and at elongation, through tryptophan  
414 stalling.

415

## 416 **DISCUSSION**

### 417 **The translational landscape of the response to multiple stresses**

418 We present a genome-wide analysis of the translational response of the fission yeast *S.*  
419 *pombe* to five different stresses using highly standardized and comparable conditions. We  
420 found that heavy metal exposure, heat shock and oxidative stress led to stronger  
421 transcriptional and translational changes than DNA damage and osmotic stress. Moreover,  
422 increased levels of eIF2 $\alpha$  phosphorylation correlate with pronounced global downregulation of  
423 translation and with strong induction of *fil1* translation. Of course, as we monitored a single  
424 time point and condition for each stress, the conclusions about the relative strength of the  
425 effects are only valid to the specific experimental conditions used. Despite this caveat, our  
426 results indicate that the translational response to stress is mainly directed to repress the  
427 translational machinery, with few genes upregulated at this level. Moreover, we found that  
428 many differentially translated genes are often regulated in multiple stresses. Thus, our study  
429 identifies the key players of a stress response at the translational level and provides insight  
430 into the biological response to stress.

431

### 432 **Fil1 regulation and role in stress responses**

433 The induction of the Fil1 transcription factor in multiple stress conditions in rich medium was  
434 surprising, as Fil1 is a master regulator of the amino acid starvation response (analogous to  
435 Gcn4 and Atf4), and is required to maintain a normal growth rate in minimal medium [12].  
436 Cells lacking Fil1 showed similar growth than wild type cells in rich medium, suggesting that  
437 Fil1 does not have a role in unstressed cells in rich medium. Strikingly, the *fil1* gene showed  
438 much higher translational induction upon cadmium, heat shock and H<sub>2</sub>O<sub>2</sub> in rich medium than  
439 in amino acid starvation induced by 3-AT in minimal medium (17-fold, 12-fold, 13-fold and 3.8-

440 fold, respectively). A possible explanation is that *fil1* translation levels may already be higher  
441 in minimal medium in unstressed cells. Similarly, the induction of the Fil1 orthologue in *S.*  
442 *cerevisiae* (Gcn4) has been reported not only in amino acid starvation or glucose limitation,  
443 but also after MMS (although the conditions were different from the ones used in this work)  
444 and H<sub>2</sub>O<sub>2</sub> treatments [33,34,53]. These results suggest that metabolic adaptation, mediated  
445 by translationally controlled transcription factors such as Fil1 and Gcn4, is an evolutionary  
446 conserved part of many stress responses (and not just amino acid starvation).

447 Fil1-dependent genes are mostly related to amino acid metabolism and transmembrane  
448 transport, and show a significant overlap with CESR induced genes. In rich medium, cells  
449 lacking Fil1 are unable to regulate the expression of Fil1 targets after cadmium, heat shock  
450 and H<sub>2</sub>O<sub>2</sub> treatments. In addition, this regulation is also impaired in *eIF2 $\alpha$ -S52A* cells,  
451 consistent with the complete absence of *fil1* induction. Surprisingly, Fil1 and its targets were  
452 upregulated in *sty1* $\Delta$  cells (compared to wild type) in unstressed conditions, possibly because  
453 the lack of a normal transcriptional response in these cells may lead to stress [14]. Moreover,  
454 it has been described that *sty1* $\Delta$  cells are sensitive to stress [45–48]. This may also reflect  
455 that Sty1 may have a role in the modulation of eIF2 $\alpha$  kinases after stress. Indeed, *sty1* $\Delta$  cells  
456 show increased eIF2 $\alpha$  phosphorylation after oxidative stress, which might result in induction  
457 of Fil1 [10,21]. Given that Sty1 is also important in adaptation to stress and that nothing is  
458 known about Fil1 protein stability or post-translational modifications, it could be also involved  
459 in downregulation of Fil1 after stress.

460 Strikingly, upon cadmium treatment, despite the induction of Fil1, the expression of Fil1-  
461 dependent genes in wild-type cells is very weak and *fil1* $\Delta$  cells are resistant to this stress.  
462 Cadmium stress increase ROS and intracellular oxidative stress [42], but the response is very  
463 different to H<sub>2</sub>O<sub>2</sub> treatment. For example, cadmium is imported through specific transporters,  
464 whereas H<sub>2</sub>O<sub>2</sub> freely diffuses into cells. Moreover, H<sub>2</sub>O<sub>2</sub> converts into superoxide, and is a  
465 substrate for the peroxiredoxin system that is responsible for the oxidation of most proteins.  
466 Indeed, *S. pombe* cells lacking transcription factors like Atf1 or Prr1 are sensitive to H<sub>2</sub>O<sub>2</sub>, but  
467 resistant or insensitive to cadmium [39,54]. Additionally, it was reported that Fil1 might drive  
468 the response to amino acid starvation partially through the action of downstream transcription  
469 factors [12]. Thus, different kinetics in the induction and the expression of Fil1-dependent  
470 genes suggest that Fil1 might be modulating transcriptional changes depending on the stress  
471 through other transcription factors. We propose that Fil1 acts as a master regulator of several  
472 stress conditions, promoting a distinct response for each situation. Further work will be  
473 required to unveil the direct targets of Fil1 under each stress condition, and whether Fil1 can  
474 activated them in different ways to modulate specific responses.

475

476 **Ribosomes stall on tryptophan codons upon H<sub>2</sub>O<sub>2</sub> treatment**

477 Ribo-seq experiments revealed that oxidative stress caused ribosome stalling on tryptophan  
478 codons, which correlated with decreased levels of charged tRNA-Trp. By contrast,  
479 intracellular levels of tryptophan were not changed significantly under these conditions,  
480 suggesting that tryptophan metabolism is not directly affected by the stress. This suggests  
481 that changes in tRNA modifications, which are poorly described in *S. pombe*, or in the tRNA-  
482 Trp synthetase activity, may affect the levels of charged tRNA-Trp and cause stalling.

483 The main eIF2 $\alpha$  kinase activated in response to early exposure to H<sub>2</sub>O<sub>2</sub> in *S. pombe* is Gcn2  
484 [10]. The molecular pathway leading to activation of Gcn2 upon nutrition limitation is well  
485 understood: Gcn2 is activated by uncharged tRNAs, which bind the histidyl-tRNA synthetase-  
486 related domain of Gcn2 at the C-terminus [55–57]. However, Gcn2 is activated by other  
487 stresses that are not expected to cause uncharged tRNA accumulation [52], such as UV  
488 irradiation or oxidative stress. Under these conditions, the tRNA binding domain of Gcn2 is  
489 still required for its activation [52]. Here, we provide evidence for the first time that a nutrient-  
490 unrelated stress like oxidative stress causes uncharged tRNA accumulation. In addition, we  
491 show that eIF2 $\alpha$  phosphorylation after oxidative stress correlates with uncharged tRNA-Trp  
492 accumulation; addition of tryptophan results in a reduction in the levels of both uncharged  
493 tRNA-Trp and of eIF2 $\alpha$  phosphorylation. Thus, we propose that the accumulation of  
494 uncharged tRNA-Trp upon oxidative stress, which causes a mild elongation defect, is used to  
495 regulate initiation through Gcn2 activation.

496

497

## 498 **METHODS**

499 **Strains, Growth Conditions, and Experimental Design.** All strains used were  
500 prototrophic. Table S1 presents a full list of strains. Standard methods and media were used  
501 for *S. pombe* [58]. For all genome-wide stress experiments, *S. pombe* cells were grown in  
502 YES medium (supplemented with leucine, uracil and adenine) at 32 °C. Cells were treated  
503 for 15 minutes as described below. Heavy metal stress: cadmium sulphate (CdSO<sub>4</sub>; 481882;  
504 Sigma) was added to a final concentration of 0.5 mM. Oxidative stress: hydrogen peroxide  
505 (H<sub>2</sub>O<sub>2</sub>; H1009; Sigma) was added to a final concentration 0.5 mM. Heat stress: cells were  
506 quickly transferred from 32°C to a prewarmed flask in a 39°C water bath. Alkylating agent:  
507 methyl methanesulfonate (MMS, 129925, Sigma) at a final concentration of 0.02%. Osmotic  
508 stress: cells were grown to OD<sub>600</sub> = 0.7, and diluted with prewarmed YES 3 M sorbitol (BP-  
509 439-500, Fisher) to a final concentration 1 M sorbitol.

510 For plate drop assays, cells were grown in YES to exponential phase at 32 °C and plated in  
511 10-fold dilutions. Plates were incubated for two days at 32 °C (except the plate incubated at  
512 39 °C for heat shock assays). For tryptophan charging experiments, supplemental tryptophan  
513 (DOC0188, Formedium) was added to the culture from a stock 8 g/L in YES to a final  
514 concentration of 200 mg/L.

515 All repeats of genome-wide experiments were independent biological replicates carried out  
516 on separate days (see ArrayExpress deposition footnote for a complete list). The following  
517 sequencing experiments were performed: (i) ribosome profiling and matching RNA-seq in five  
518 stress conditions of three strains (wild-type, *eIF2α-S52A* and *sty1Δ*), and (ii) RNA-seq of *fil1Δ*  
519 and cells in five stress conditions.

520

521 **Amino acid analysis.** Amino acid quantification was performed by liquid chromatography  
522 selective reaction monitoring (LC-SRM) as described [59].

523

524 **Protein Analyses.** To prepare samples for Western blotting, cells were harvested by  
525 filtration, washed with 20% TCA, resuspended in 100 µL of 20% TCA, and frozen. Cell pellets  
526 were lysed with 1 mL of acid-treated glass beads in a bead beater (FastPrep-5; MP  
527 Biomedicals) at level 7.5 for 15 s, and 400 µL of 5% TCA was added before eluting from the  
528 glass beads. Lysates were frozen on dry ice and spun at 18,000 relative centrifugal force for  
529 10 min. Pellets were resuspended in SDS-Tris solution (2% SDS and Tris 0.3M pH 10.7),  
530 boiled during 5 min and cleared by centrifugation at maximum speed for 2 min. Protein extract  
531 concentrations were measured using Pierce BCA Protein Assay solution (Thermo), and 60-  
532 90 µg of total protein were loaded with Laemmli SDS Sample Buffer (reducing) (Alfa Aesar).  
533 For western blot analysis, the following antibodies were used: anti-eIF2α (1:500; 9722, Cell



534 Signalling), anti-Phospho-eIF2 $\alpha$  (1:1,000; 9721, Cell Signalling), and anti-tubulin (1:10,000;  
535 sc-23948, Santa Cruz). The secondary antibodies were HRP-conjugated goat anti-mouse IgG  
536 (H+L) (1:10,000; 31430, Thermo Fisher) and anti-rabbit IgG (1:10,000; ab-6721, Abcam). TAP  
537 tag was detected with peroxide-anti-peroxide complexes (P1291; Sigma). Detection was  
538 performed using the enhanced chemiluminescence procedure (ECL kit).

539

540 **Northern analysis of aminoacyl-tRNA charging.** RNA from the indicated conditions  
541 was prepared by phenol extraction under acidic conditions using acid buffer (0.3 M sodium  
542 acetate pH 5, 10 mM Na<sub>2</sub>EDTA) for resuspension of frozen cells, and final acid RNA buffer  
543 (10 mM sodium acetate pH 5, 1mM EDTA). As control samples, RNA was deacylated with  
544 0.2 M Tris pH 9.0 for 2h at 37 °C. Periodate oxidation and  $\beta$ -elimination were performed as  
545 described [51] using 2  $\mu$ g of total RNA. In the final step, all samples were deacylated. tRNAs  
546 were detected by Northern blotting in non-acidic conditions: RNA samples were loaded onto  
547 a 6.5 % denaturing urea polyacrylamide gel, electrophoresed at 17 W for 70 min and  
548 transferred onto an Amersham Hybond-N membrane (GE Healthcare) using the Trans-blot  
549 SD semi-dry transfer cell (Biorad) as described [60], but using non-acidic conditions. The  
550 oligonucleotide probes used were: tRNA Trp CCA (5'-  
551 TGACCCCTAAGTGACTTGAACACTTGA-3'), tRNA His GUG (5'-  
552 TGCCCACACCAGGAATCGAACCTGGGT-3') and U5 snRNA as loading control (5'-  
553 GCACACCTTACAAACGGCTGTTTCTG-3') [51]. The oligonucleotides were labelled with  
554 infrared dyes (IRD-700 or IRD-800) at the 5' end for fluorescence detection using the LICOR  
555 Odyssey system. The tRNA loading was quantified as the ratio of upper to lower bands relative  
556 to the unstressed condition.

557

558 **Polysome profiling, ribosome profiling, library preparation and sequencing.**

559 Ribosome-protected fragment (RPF) analyses, preparation of cell extracts, RNase treatment,  
560 separation of samples by centrifugation through sucrose gradients, and isolation of protected  
561 RNA fragments were performed as described [61]. For polysome profiles, there is no RNase  
562 I digestion step, and lysis buffer and sucrose solutions were prepared with double  
563 concentration of MgCl<sub>2</sub> (10 mM). Polysome-subpolysome ratio was quantified by measuring  
564 the area under the curve relative to the unstressed conditions using Image J software (NIH).

565 For all RPF samples, gel-purified RNA fragments of around 17-30 nucleotides were treated  
566 with 10 units of T4 PNK (Thermo Fisher) in a low-pH buffer (700 mM Tris, pH 7, 50 mM DTT,  
567 and 100 mM MgCl<sub>2</sub>) for 30 min at 37 °C. ATP and buffer A (Thermo Fisher) were then added  
568 for an additional 30 min incubation. RNA fragments were column-purified (PureLink RNA  
569 microcolumns; Life Technologies). A total of 100 ng was used as input for the NEXTFLEX

570 Small RNA Sequencing Kit (Version 3; Bioo Scientific), and libraries were generated following  
571 the manufacturer's protocol. For mRNA analyses, total RNA was isolated as described [61].  
572 Total RNA was then depleted from rRNA by using Ribo-Zero Gold rRNA Removal Kit Yeast  
573 (Illumina) with 4  $\mu$ g as input. Finally, 30 ng of rRNA-depleted RNA was used as starting  
574 material for the NEXTflex Rapid Directional qRNA-Seq Kit (Bioo Scientific). Libraries were  
575 sequenced in an Illumina HiSeq4000 or Novaseq6000 as indicated (ArrayExpress  
576 submission).

577

578 **Data Analysis.** Data processing and read alignment were performed as described [12].  
579 Data quantification (number of reads per coding sequence) was carried out by using in-house  
580 Perl scripts as described [12]. All statistical analyses were performed using R.

581 Differential expression analysis was performed by using the Bioconductor DESeq2 package  
582 [62]. Raw counts were directly fed to the program, and no filtering was applied. Unless  
583 otherwise indicated, a threshold of  $10^{-2}$  was chosen for the adjusted P value, and a cut-off of  
584 2-fold minimal change in RNA levels.

585 For codon usage analyses, RPF reads were aligned to nucleotide 13 (corresponding to  
586 position 1 of the codon in the ribosome P site). Only codons after 90 were used. For each  
587 coding sequence, the following calculations were performed: (i) determination of the fraction  
588 of RPFs that occupy each codon (RPFs in a given codon divided by total RPFs); (ii)  
589 quantification of the relative abundance of each codon on the coding sequence (number of  
590 times each codon is present divided by total codon number); and (iii) definition of the  
591 normalized codon occupancy by dividing parameter 1 by parameter 2. The average codon  
592 enrichments (Fig. 5, S4) were then calculated with data from all coding sequences.

593 For the analysis of translational efficiencies we used RiboDiff [63]. RiboDiff was provided  
594 with raw read counts for each gene, from ribosome profiling and from RNA-seq. To select  
595 differentially translated genes, a threshold of  $10^{-2}$  for the adjusted P value, and a cut-off of  
596 1.5-fold were chosen.

597 Translation efficiency and mRNA ratios were median-centred for plotting. The list of Fil1  
598 targets for Figures 4 and S3 was obtained from, Dataset\_S01, repressed genes in *fil1 $\Delta$*  versus  
599 wild type without stress (no 3AT) [12] and only those genes from the lists with at least 20  
600 counts in 80% or more samples were used. Gene set enrichment was performed with AnGeLi  
601 [64]. The significance of the overlap between gene lists was calculated using Fisher's exact  
602 test.

603

604 **Data availability.** All raw data files have been deposited in ArrayExpress [65]  
605 [<https://www.ebi.ac.uk/arrayexpress/>] under accessions: E-MTAB-8746, E-MTAB-8686, E-  
606 MTAB-8744, E-MTAB-8745, E-MTAB-8602 and E-MTAB-8583.

607

## 608 **ACKNOWLEDGMENTS**

609 This work was supported by a Biotechnology and Biological Sciences (BBSRC) grant to Juan  
610 Mata (BB/N007697/1). Markus Ralser was supported by the Francis Crick Institute, which  
611 receives its core funding from Cancer Research UK (FC001134), the UK Medical Research  
612 Council (FC001134), and the Wellcome Trust (FC001134), as well as specific project funding  
613 from the Wellcome Trust (IA 200829/Z/16/Z to M.R.), as well as the German Federal Ministry  
614 of Education and Research (BMBF) as part of the National Research Node Mass  
615 Spectrometry in Systems Medicine (MSCoreSys 031L0220A). We thank Samuel Marguerat  
616 and Caia Duncan for comments on the manuscript and Mathew Peacey and Anno Koetje for  
617 help with experiments.

618

## 619 **AUTOR CONTRIBUTIONS**

620 A.R., S.G. and J.M. designed the study. A.R., S.G. and M.M. performed and analysed  
621 experiments. A.R., M.R. and J.M. analysed data. A.R. and J.M. wrote the manuscript.

622

## 623 **CONFLICT OF INTEREST**

624 The authors declare no competing financial interest.

625

626 **Table S1: Strain and experiment list**

Genotype	Origin	Reference	Usage
972 h-	Lab collection	JU96	Ribo-seq, RNA-seq, drop assay, eIF2 $\alpha$ phosphorylation
<i>eIF2<math>\alpha</math>-S52A::ura4<sup>+</sup> h-</i>	Sandra López-Avilés	JU1502	Ribo-seq, eIF2 $\alpha$ phosphorylation
<i>sty1::ura4<sup>+</sup> ura4D18 h-</i>	Sandra López-Avilés, <i>crossed out markers</i>	JU1503	Ribo-seq, eIF2 $\alpha$ phosphorylation
<i>fil1::kanMX6 h-</i>	Lab collection	JU1594	RNA-seq, drop assay
<i>fil1:TAP h+</i>	Lab collection	JU1525	Fil1 expression
<i>fil1:TAP eIF2<math>\alpha</math> S52A::ura4<sup>+</sup> h-</i>	This work	JU1865	Fil1 expression
<i>fil1:TAP::CRISPR sty1::ura4<sup>+</sup> h-</i>	This work	JU1749	Fil1 expression

## 627 REFERENCES

- 628 1. Spriggs KA, Bushell M, Willis AE. Translational Regulation of Gene Expression during  
629 Conditions of Cell Stress. *Mol Cell*. 2010;40: 228–237.  
630 doi:10.1016/j.molcel.2010.09.028
- 631 2. Lindqvist LM, Tandoc K, Topisirovic I, Furic L. Cross-talk between protein synthesis,  
632 energy metabolism and autophagy in cancer. *Curr Opin Genet Dev*. 2018;48: 104–  
633 111. doi:10.1016/j.gde.2017.11.003
- 634 3. Tahmasebi S, Khoutorsky A, Mathews MB, Sonenberg N. Translation deregulation in  
635 human disease. *Nat Rev Mol Cell Biol*. 2018;19: 791–807. doi:10.1038/s41580-018-  
636 0034-x
- 637 4. Sonenberg N, Hinnebusch AG. Regulation of Translation Initiation in Eukaryotes:  
638 Mechanisms and Biological Targets. *Cell*. 2009;136: 731–745.  
639 doi:10.1016/j.cell.2009.01.042
- 640 5. Pavitt GD, Ramaiah KVA, Kimball SR, Hinnebusch AG. eIF2 independently binds two  
641 distinct eIF2b subcomplexes that catalyze and regulate guanine-nucleotide exchange.  
642 *Genes Dev*. 1998;12: 514–526. doi:10.1101/gad.12.4.514
- 643 6. Dever TE, Kinzy TG, Pavitt GD. Mechanism and regulation of protein synthesis in  
644 *Saccharomyces cerevisiae*. *Genetics*. 2016;203: 65–107.  
645 doi:10.1534/genetics.115.186221
- 646 7. Dever TE, Feng L, Wek RC, Cigan AM, Donahue TF, Hinnebusch AG.  
647 Phosphorylation of initiation factor 2 $\alpha$  by protein kinase GCN2 mediates gene-specific  
648 translational control of GCN4 in yeast. *Cell*. 1992;68: 585–596. doi:10.1016/0092-  
649 8674(92)90193-G
- 650 8. Hinnebusch AG. Translational Regulation of Gcn4 and the General Amino Acid  
651 Control of Yeast. *Annu Rev Microbiol*. 2005;59: 407–450.  
652 doi:10.1146/annurev.micro.59.031805.133833
- 653 9. Zhan K, Narasimhan J, Wek RC. Differential activation of eIF2 kinases in response to  
654 cellular stresses in *Schizosaccharomyces pombe*. *Genetics*. 2004;168: 1867–1875.  
655 doi:10.1534/genetics.104.031443
- 656 10. Berlanga JJ, Rivero D, Martín R, Herrero S, Moreno S, De Haro C. Role of Mitogen-  
657 Activated Protein Kinase Sty1 in Regulation of Eukaryotic Initiation Factor 2 $\alpha$  Kinases  
658 in Response to Environmental Stress in *Schizosaccharomyces pombe*. *Eukaryot Cell*.  
659 2010;9: 194–207. doi:10.1128/EC.00185-09
- 660 11. Martin R, Berlanga JJ, de Haro C. New roles of the fission yeast eIF2 kinases Hri1  
661 and Gcn2 in response to nutritional stress. *J Cell Sci*. 2013;126: 3010–3020.  
662 Available: <http://jcs.biologists.org/cgi/doi/10.1242/jcs.118067>

- 663 12. Duncan CDS, Rodríguez-López M, Ruis P, Bähler J, Mata J. General amino acid  
664 control in fission yeast is regulated by a nonconserved transcription factor, with  
665 functions analogous to Gcn4/Atf4. *Proc Natl Acad Sci*. 2018;115: E1829–E1838.  
666 doi:10.1073/pnas.1713991115
- 667 13. Vatter KM, Wek RC. Reinitiation involving upstream ORFs regulates ATF4 mRNA  
668 translation in mammalian cells. *Proc Natl Acad Sci U S A*. 2004;101: 11269–11274.  
669 doi:10.1073/pnas.0400541101
- 670 14. Chen D, Toone WM, Mata J, Lyne R, Burns G, Kivinen K, et al. Global transcriptional  
671 responses of fission yeast to environmental stress. *Mol Biol Cell*. 2003;14: 214–29.  
672 doi:10.1091/mbc.e02-08-0499
- 673 15. Chen D, Wilkinson CRM, Watt S, Penkett CJ, Toone WM, Jones N, et al. Multiple  
674 Pathways Differentially Regulate Global Oxidative Stress Responses in Fission Yeast.  
675 *Mol Biol Cell*. 2008;19: 308–317. doi:10.1091/mbc.E07
- 676 16. Toone WM, Jones N. Stress-activated signalling pathways in yeast. *Genes to Cells*.  
677 1998;3: 485–498. doi:10.1046/j.1365-2443.1998.00211.x
- 678 17. Shiozaki K, Russell P. Conjugation, meiosis, and the osmotic stress response are  
679 regulated by Spc1 kinase through Atf1 transcription factor in fission yeast. *Genes*  
680 *Dev*. 1996;10: 2276–2288. doi:10.1101/gad.10.18.2276
- 681 18. Wilkinson MG, Samuels M, Takeda T, Mark Toone W, Shieh JC, Toda T, et al. The  
682 Atf1 transcription factor is a target for the Sty1 stress-activated MAP kinase pathway  
683 in fission yeast. *Genes Dev*. 1996;10: 2289–2301. doi:10.1101/gad.10.18.2289
- 684 19. Gaits F, Degols G, Shiozaki K, Russell P. Phosphorylation and association with the  
685 transcription factor Atf1 regulate localization of Spc1/Sty1 stress-activated kinase in  
686 fission yeast. *Genes Dev*. 1998;12: 1464–1473. doi:10.1101/gad.12.10.1464
- 687 20. Perez P, Cansado J. Cell Integrity Signaling and Response to Stress in Fission Yeast.  
688 *Curr Protein Pept Sci*. 2010;11: 680–692. doi:10.2174/138920310794557718
- 689 21. Dunand-Sauthier I, Walker CA, Narasimhan J, Pearce AK, Wek RC, Humphrey TC.  
690 Stress-activated protein kinase pathway functions to support protein synthesis and  
691 translational adaptation in response to environmental stress in fission yeast. *Eukaryot*  
692 *Cell*. 2005;4: 1785–1793. doi:10.1128/EC.4.11.1785-1793.2005
- 693 22. Asp E, Nilsson D, Sunnerhagen P. Fission yeast mitogen-activated protein kinase  
694 Sty1 interacts with translation factors. *Eukaryot Cell*. 2008;7: 328–338.  
695 doi:10.1128/EC.00358-07
- 696 23. Pan T. Modifications and functional genomics of human transfer RNA. *Cell Research*.  
697 Nature Publishing Group; 2018. pp. 395–404. doi:10.1038/s41422-018-0013-y
- 698 24. Jackman JE, Alfonzo JD. Transfer RNA modifications: nature’s combinatorial  
699 chemistry playground. *Wiley Interdiscip Rev RNA*. 2013;4: 35–48.

- 700 doi:10.1002/wrna.1144
- 701 25. Kadaba S, Krueger A, Trice T, Krecic AM, Hinnebusch AG, Anderson J. Nuclear  
702 surveillance and degradation of hypomodified initiator tRNA<sup>Met</sup> in *S. cerevisiae*.  
703 *Genes Dev.* 2004;18: 1227–40. doi:10.1101/gad.1183804
- 704 26. Patil A, Chan CTY, Dyavaiah M, Rooney JP, Dedon PC, Begley TJ. Translational  
705 infidelity-induced protein stress results from a deficiency in Trm9-catalyzed tRNA  
706 modifications. *RNA Biol.* 2012;9: 990–1001. doi:10.4161/rna.20531
- 707 27. Thompson DM, Lu C, Green PJ, Parker R. tRNA cleavage is a conserved response to  
708 oxidative stress in eukaryotes. *RNA.* 2008;14: 2095–2103. doi:10.1261/rna.1232808
- 709 28. Ivanov P, Emara MM, Villen J, Gygi SP, Anderson P. Angiogenin-induced tRNA  
710 fragments inhibit translation initiation. *Mol Cell.* 2011;43: 613–23.  
711 doi:10.1016/j.molcel.2011.06.022
- 712 29. Ingolia NT, Ghaemmaghami S, Newman JRS, Weissman JS. Genome-wide analysis  
713 in vivo of translation with nucleotide resolution using ribosome profiling. *Science.*  
714 2009;324: 218–223. doi:10.1126/science.1168978
- 715 30. Duncan CDS, Mata J. Effects of cycloheximide on the interpretation of ribosome  
716 profiling experiments in *Schizosaccharomyces pombe*. *Sci Rep.* 2017;7: 10331.  
717 doi:10.1038/s41598-017-10650-1
- 718 31. Gerashchenko M V., Lobanov A V., Gladyshev VN. Genome-wide ribosome profiling  
719 reveals complex translational regulation in response to oxidative stress. *Proc Natl*  
720 *Acad Sci U S A.* 2012;109: 17394–17399. doi:10.1073/pnas.1120799109
- 721 32. Lackner DH, Beilharz TH, Marguerat S, Mata J, Watt S, Schubert F, et al. A network  
722 of multiple regulatory layers shapes gene expression in fission yeast. *Mol Cell.*  
723 2007;26: 145–55. doi:10.1016/j.molcel.2007.03.002
- 724 33. Claire Mascarenhas, Laura C. Edwards-Ingram, Leo Zeef, Daniel Shenton, Mark P.  
725 Ashe and CMG. Gcn4 Is Required for the Response to Peroxide Stress in the Yeast  
726 *Saccharomyces cerevisiae*. *Mol Biol Cell.* 2008;19: 2995–3007. doi:10.1091/mbc.E07
- 727 34. Natarajan K, Meyer MR, Jackson BM, Slade D, Roberts C, Hinnebusch AG, et al.  
728 Transcriptional Profiling Shows that Gcn4p Is a Master Regulator of Gene Expression  
729 during Amino Acid Starvation in Yeast. *Mol Cell Biol.* 2001;21: 4347–4368.  
730 doi:10.1128/MCB.21.13.4347-4368.2001
- 731 35. Shenton D, Smirnova JB, Selley JN, Carroll K, Hubbard SJ, Pavitt GD, et al. Global  
732 translational responses to oxidative stress impact upon multiple levels of protein  
733 synthesis. *J Biol Chem.* 2006;281: 29011–29021. doi:10.1074/jbc.M601545200
- 734 36. Preiss T, Baron-Benhamou J, Ansorge W, Hentze MW. Homodirectional changes in  
735 transcriptome composition and mRNA translation induced by rapamycin and heat  
736 shock. *Nat Struct Biol.* 2003;10: 1039–1047. doi:10.1038/nsb1015

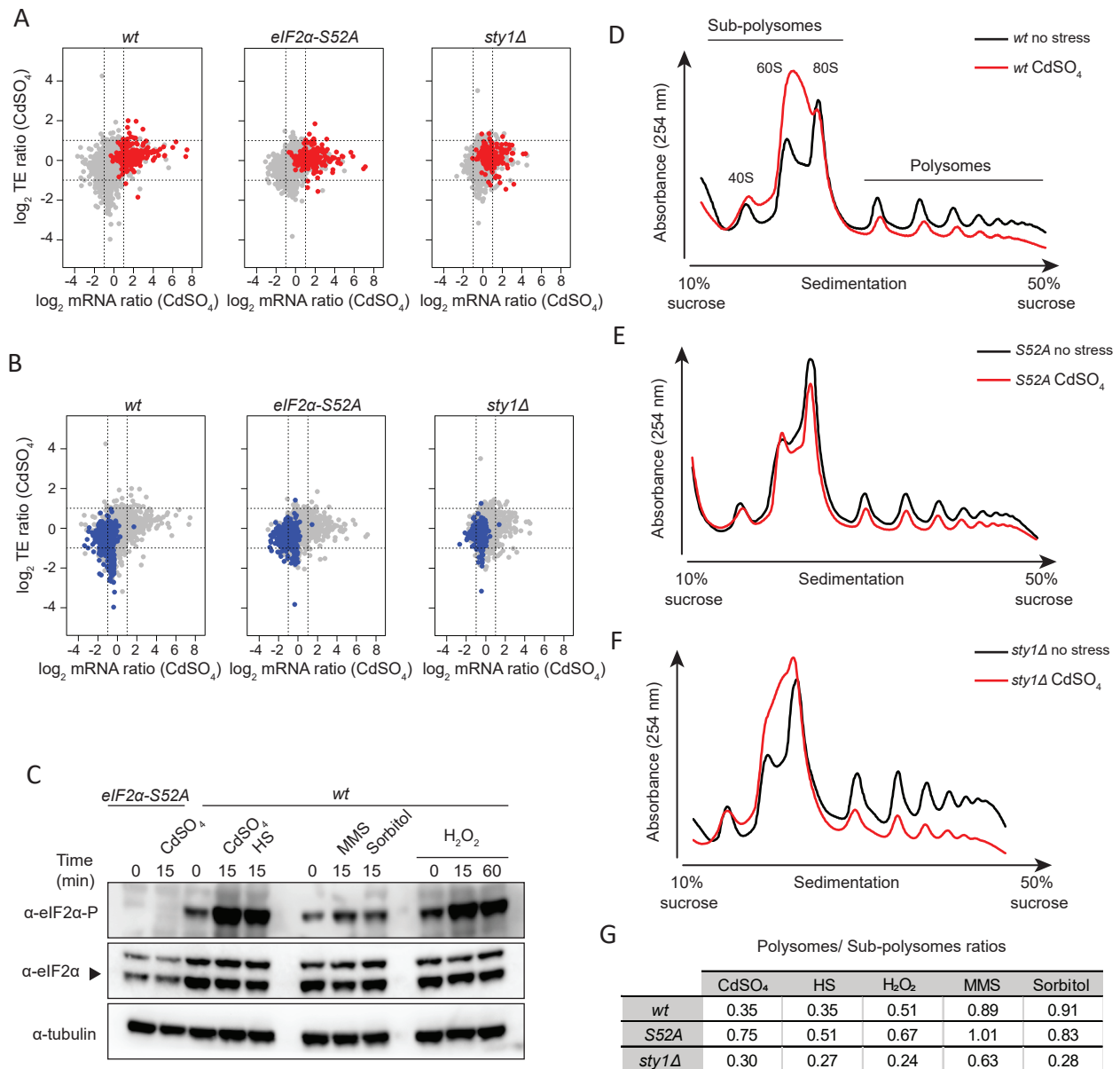
- 737 37. Knutsen JHJ, Rødland GE, Bøe CA, Håland TW, Sunnerhagen P, Grallert B, et al.  
738 Stress-induced inhibition of translation independently of eIF2 $\alpha$  phosphorylation. *J Cell*  
739 *Sci.* 2015;128: 4420–4427. doi:10.1242/jcs.176545
- 740 38. Boye E, Grallert B. eIF2 $\alpha$  phosphorylation and the regulation of translation. *Current*  
741 *Genetics.* Springer Verlag; 2019. doi:10.1007/s00294-019-01026-1
- 742 39. Ohmiya R, Kato C, Yamada H, Aiba H, Mizuno T. A fission yeast gene (*prr1+*) that  
743 encodes a response regulator implicated in oxidative stress response. *J Biochem.*  
744 1999;125: 1061–1066. doi:10.1093/oxfordjournals.jbchem.a022387
- 745 40. Nakamichi N, Yanada H, Aiba H, Aoyama K, Ohmiya R, Mizuno T. Characterization of  
746 the *prr1* response regulator with special reference to sexual development in  
747 *Schizosaccharomyces pombe*. *Biosci Biotechnol Biochem.* 2003;67: 547–555.  
748 doi:10.1271/bbb.67.547
- 749 41. Calvo IA, García P, Ayté J, Hidalgo E. The transcription factors Pap1 and Prr1  
750 collaborate to activate antioxidant, but not drug tolerance, genes in response to  
751 H<sub>2</sub>O<sub>2</sub>. *Nucleic Acids Res.* 2012;40: 4816–4824. doi:10.1093/nar/gks141
- 752 42. Cuypers A, Plusquin M, Remans T, Jozefczak M, Keunen E, Gielen H, et al.  
753 Cadmium stress: An oxidative challenge. *BioMetals.* 2010;23: 927–940.  
754 doi:10.1007/s10534-010-9329-x
- 755 43. Lackner DH, Schmidt MW, Wu S, Wolf DA, Bähler J. Regulation of transcriptome,  
756 translation, and proteome in response to environmental stress in fission yeast.  
757 *Genome Biol.* 2012;13: R25. doi:10.1186/gb-2012-13-4-r25
- 758 44. Kanoh J, Russell P. The protein kinase Cdr2, related to Nim1/Cdr1 mitotic inducer,  
759 regulates the onset of mitosis in fission yeast. *Mol Biol Cell.* 1998;9: 3321–3334.  
760 doi:10.1091/mbc.9.12.3321
- 761 45. Millar JB, Buck V, Wilkinson MG. Pyp1 and Pyp2 PTPases dephosphorylate an  
762 osmosensing MAP kinase controlling cell size at division in fission yeast. *Genes Dev.*  
763 1995;9: 2117–30.
- 764 46. Shiozaki K, Russell P. Cell-cycle control linked to extracellular environment by MAP  
765 kinase pathway in fission yeast. *Nature.* 1995;378: 739–743.
- 766 47. Degols G, Shiozaki K, Russell P. Activation and regulation of the Spc1 stress-  
767 activated protein kinase in *Schizosaccharomyces pombe*. *Mol Cell Biol.* 1996;16:  
768 2870–2877. doi:10.1128/mcb.16.6.2870
- 769 48. Degols G, Russell P. Discrete roles of the Spc1 kinase and the Atf1 transcription  
770 factor in the UV response of *Schizosaccharomyces pombe*. *Mol Cell Biol.* 1997;17:  
771 3356–3363. doi:10.1128/mcb.17.6.3356
- 772 49. Greenall A, Hadcroft AP, Malakasi P, Jones N, Morgan BA, Hoffman CS, et al. Role of  
773 fission yeast Tup1-like repressors and Prr1 transcription factor in response to salt



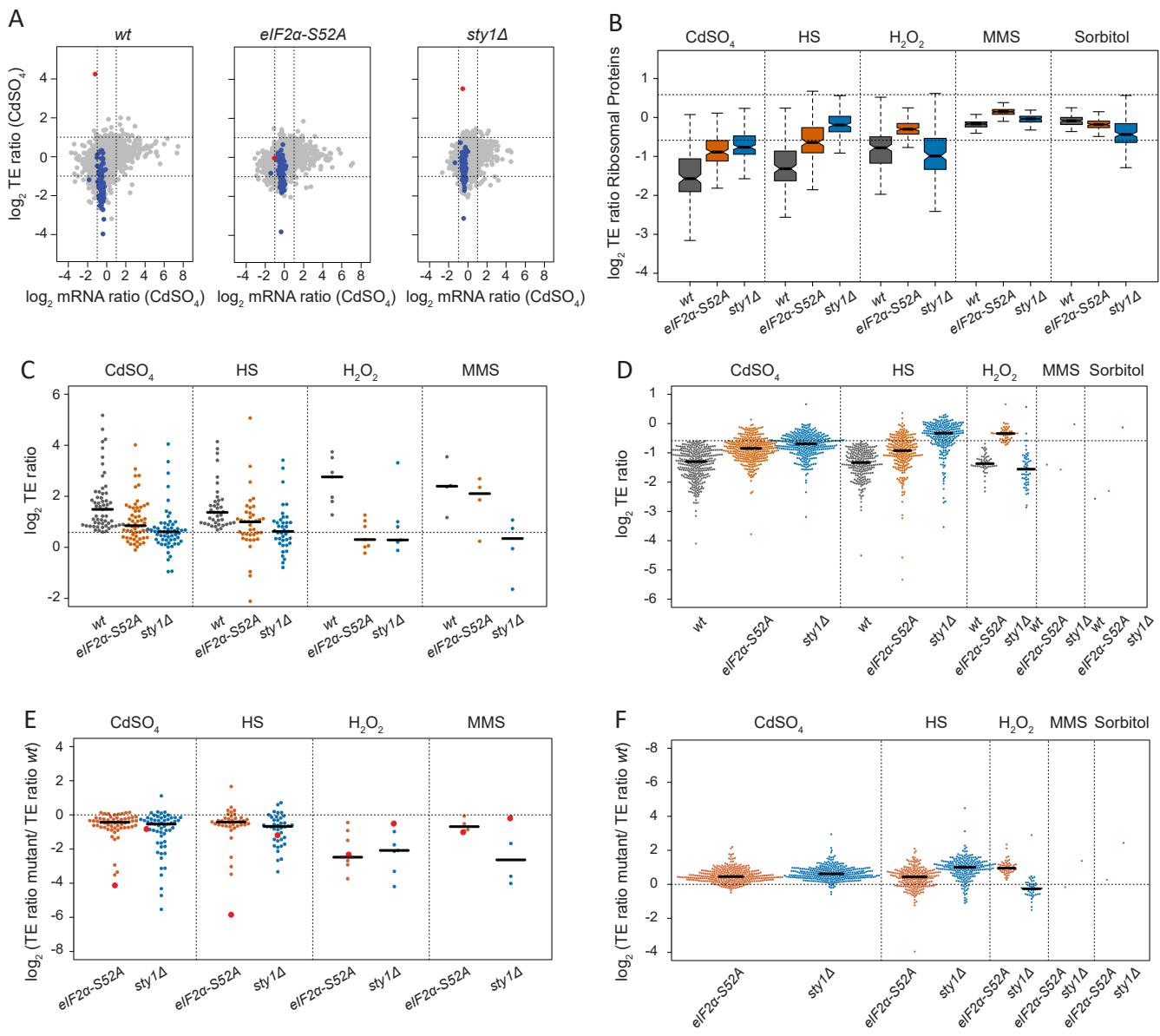
- 774 stress. *Mol Biol Cell*. 2002;13: 2977–89. doi:10.1091/mbc.01-12-0568
- 775 50. Hasan A, Cotobal C, Duncan CDS, Mata J, Copenhaver GP. Systematic Analysis of  
776 the Role of RNA-Binding Proteins in the Regulation of RNA Stability. *PLoS Genet*.  
777 2014;10. doi:10.1371/journal.pgen.1004684
- 778 51. Vakiloroyaei A, Shah NS, Oeffinger M, Bayfield MA. The RNA chaperone La  
779 promotes pre-tRNA maturation via indiscriminate binding of both native and  
780 misfolded targets. *Nucleic Acids Res*. 2017;45: 11341–11355. doi:10.1093/nar/gkx764
- 781 52. Anda S, Zach R, Grallert B. Activation of Gcn2 in response to different stresses. *PLoS*  
782 *One*. 2017;12: e0182143. doi:10.1371/journal.pone.0182143
- 783 53. Yang R, Wek SA, Wek RC. Glucose Limitation Induces GCN4 Translation by  
784 Activation of Gcn2 Protein Kinase. *Mol Cell Biol*. 2000;20: 2706–2717.  
785 doi:10.1128/mcb.20.8.2706-2717.2000
- 786 54. Guo L, Ganguly A, Sun L, Suo F, Du L-L, Russell P. Global Fitness Profiling Identifies  
787 Arsenic and Cadmium Tolerance Mechanisms in Fission Yeast. *G3 (Bethesda)*.  
788 2016;6: 3317–3333. doi:10.1534/g3.116.033829
- 789 55. Dong J, Qiu H, Garcia-Barrio M, Anderson J, Hinnebusch AG. Uncharged tRNA  
790 activates GCN2 by displacing the protein kinase moiety from a bipartite tRNA-binding  
791 domain. *Mol Cell*. 2000;6: 269–279. doi:10.1016/S1097-2765(00)00028-9
- 792 56. Wek SA, Zhu S, Wek RC. The histidyl-tRNA synthetase-related sequence in the eIF2  
793 alpha protein kinase GCN2 interacts with tRNA and is required for activation in  
794 response to starvation for different amino acids. *Mol Cell Biol*. 1995;15: 4497–4506.  
795 doi:10.1128/mcb.15.8.4497
- 796 57. Zhu S, Sobolev AY, Wek RC. Histidyl-tRNA synthetase-related sequences in GCN2  
797 protein kinase regulate in vitro phosphorylation of eIF2. *J Biol Chem*. 1996;271:  
798 24989–24994. doi:10.1074/jbc.271.40.24989
- 799 58. Moreno S, Klar A, Nurse P. Molecular genetic analysis of fission yeast  
800 *Schizosaccharomyces pombe*. *Methods Enzymol*. 1991;194: 795–823.
- 801 59. Mülleder M, Bluemlein K, Ralser M. A high-throughput method for the quantitative  
802 determination of free amino acids in *saccharomyces cerevisiae* by hydrophilic  
803 interaction chromatography-tandem mass spectrometry. *Cold Spring Harb Protoc*.  
804 2017;2017: 729–734. doi:10.1101/pdb.prot089094
- 805 60. Janssen BD, Diner EJ, Hayes CS. Analysis of Aminoacyl- and Peptidyl-tRNAs by Gel  
806 Electrophoresis. In: Keiler KC, editor. *Bacterial Regulatory RNA: Methods and*  
807 *Protocols*. Totowa, NJ: Humana Press; 2012. pp. 291–309. doi:10.1007/978-1-61779-  
808 949-5\_19
- 809 61. Duncan CDS, Mata J. The translational landscape of fission-yeast meiosis and  
810 sporulation. *Nat Struct Mol Biol*. 2014;21: 641–647. doi:10.1038/nsmb.2843

- 811 62. Love MI, Huber W, Anders S. Moderated estimation of fold change and dispersion for  
812 RNA-seq data with DESeq2. *Genome Biol.* 2014;15. doi:10.1186/s13059-014-0550-8
- 813 63. Zhong Y, Karaletsos T, Drewe P, Sreedharan VT, Kuo D, Singh K, et al. RiboDiff:  
814 Detecting changes of mRNA translation efficiency from ribosome footprints.  
815 *Bioinformatics.* 2017;33: 139–141. doi:10.1093/bioinformatics/btw585
- 816 64. Bitton DA, Schubert F, Dey S, Okoniewski M, Smith GC, Khadayate S, et al. AnGeLi:  
817 A Tool for the Analysis of Gene Lists from Fission Yeast. *Front Genet.* 2015;6: 330.  
818 doi:10.3389/fgene.2015.00330
- 819 65. Athar A, Füllgrabe A, George N, Iqbal H, Huerta L, Ali A, et al. ArrayExpress update -  
820 from bulk to single-cell expression data. *Nucleic Acids Res.* 2019;47: D711–D715.  
821 doi:10.1093/nar/gky964
- 822
- 823

Figure 1

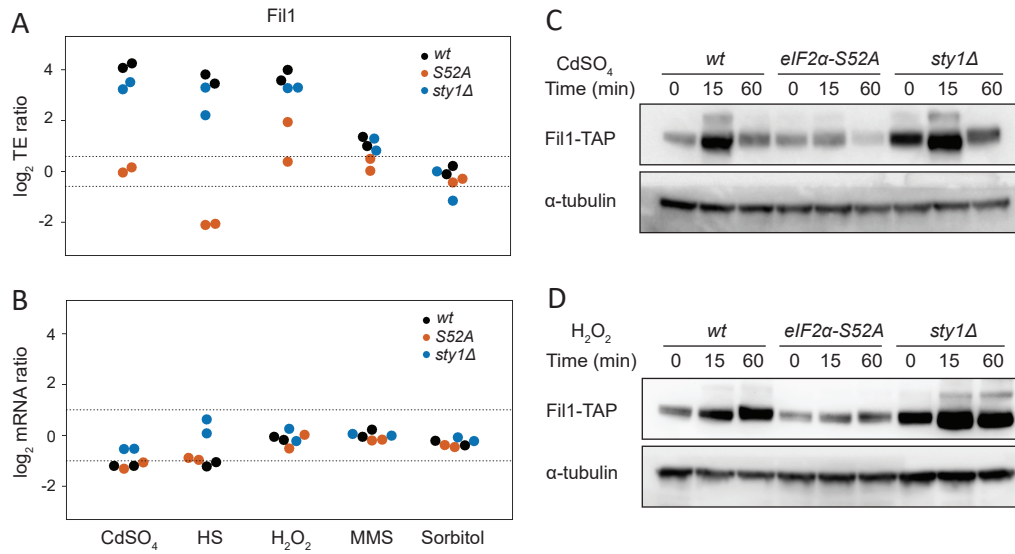


**Fig 1. General responses to stress. (A)** Scatter plot comparing mRNA levels and translation efficiencies ( $\log_2$  ratios stress/control) upon cadmium treatment (15 min) in wild type, eIF2 $\alpha$ -S52A and sty1 $\Delta$  genetic backgrounds. The results of a single experiment are shown. CCSR-induced genes are plotted in red. **(B)** As in A, but CCSR-repressed genes are plotted in blue. **(C)** Western blots comparing eIF2 $\alpha$  phosphorylation levels after the five treatments for the indicated times in wild type cells. In the first two lanes (left), eIF2 $\alpha$ -S52A cells were used as negative control for the anti-eIF2 $\alpha$  phosphorylation antibody. Tubulin was employed as a loading control. **(D to F)** Representative polysome profile traces before and after cadmium treatment (15 min) in wild type **(D)**, eIF2 $\alpha$ -S52A **(E)** and sty1 $\Delta$  cells **(F)**. **(G)** Estimation of polysome/subpolysome ratios after five stress treatments (15 min) relative to unstressed conditions.



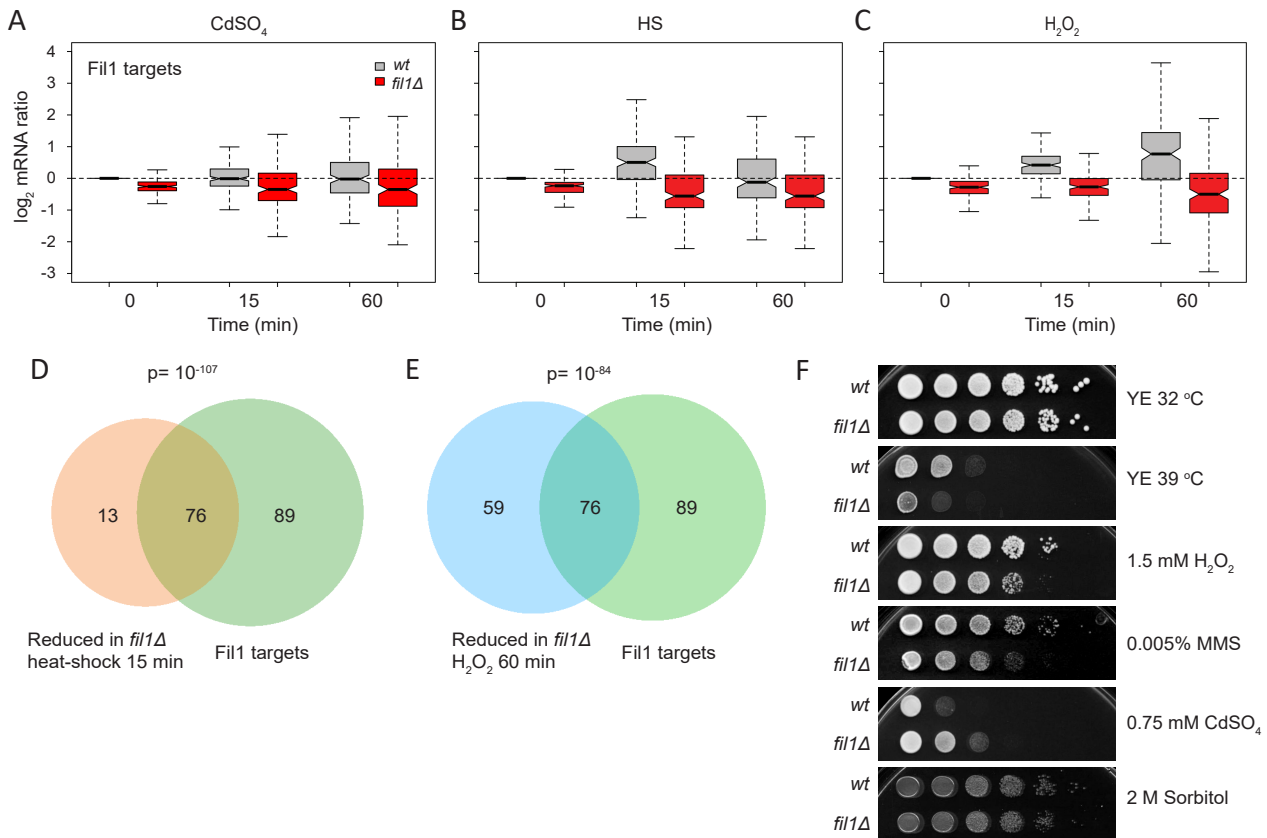
**Fig. 2. Translational regulation upon stress exposure. (A)** Scatter plot comparing mRNA levels and translation efficiencies ( $\log_2$  ratios stress/control) upon cadmium treatment (15 min) in wild type, *eIF2 $\alpha$ -S52A* and *sty1 $\Delta$*  genetic backgrounds. The results of a single experiment are shown. The *fil1* gene is plotted in red and genes encoding ribosomal proteins in blue. **(B)** Boxplots comparing translation efficiencies of stressed and control cells ( $\log_2$  ratios stress/control) of genes encoding ribosomal proteins. Data are shown for wild type, *eIF2 $\alpha$ -S52A* and *sty1 $\Delta$*  cells. **(C)** Comparisons of translation efficiencies of stressed (15 min) and control cells ( $\log_2$  ratios stress/control). Only genes that showed significant translational upregulation in wild type cells in at least one stress are displayed. Data are presented for wild type, *eIF2 $\alpha$ -S52A* and *sty1 $\Delta$*  cells. **(D)** As in C, but only genes that showed significant translational downregulation are displayed. **(E)** As in C, but TE changes have been normalised to those of wild type cells. Dots corresponding to *fil1* gene are shown in red. **(F)** As in E, but data are displayed for significantly downregulated genes.

Figure 3



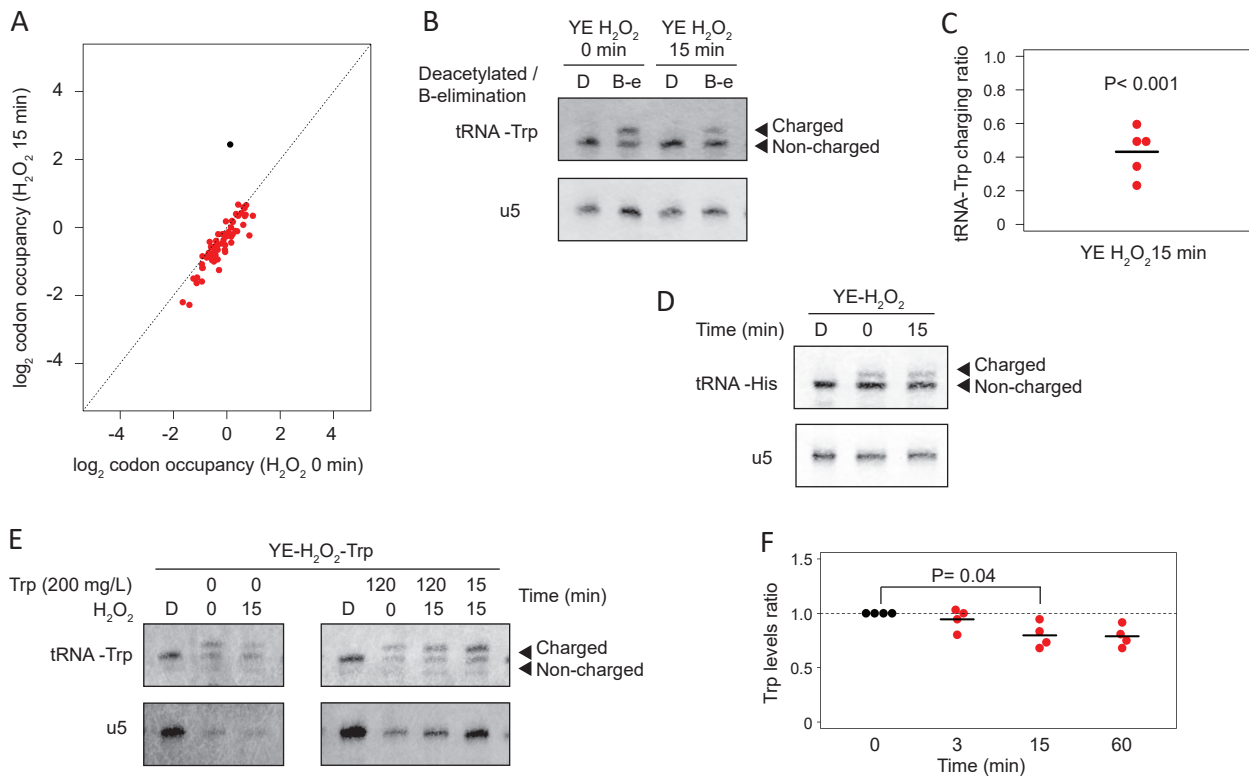
**Fig. 3. *Fil1* is the major translational responder to stress.** **(A)** Comparison of translation efficiency of the *fil1* gene between stressed and control cells ( $\log_2$  ratios stress/control). The dotted lines indicate 1.5-fold changes. Data are presented for wild type, *eIF2 $\alpha$ -S52A* and *sty1 $\Delta$*  cells. **(B)** As in C, but for *fil1* mRNA changes. The dotted lines indicate 2-fold changes **(C)** Western blots to measure Fil1-TAP protein levels after cadmium treatment for the indicated times. Data are presented for wild type, *eIF2 $\alpha$ -S52A* and *sty1 $\Delta$*  cells. Tubulin was used as a loading control. **(D)** As in C, but after  $H_2O_2$  treatment.

Figure 4

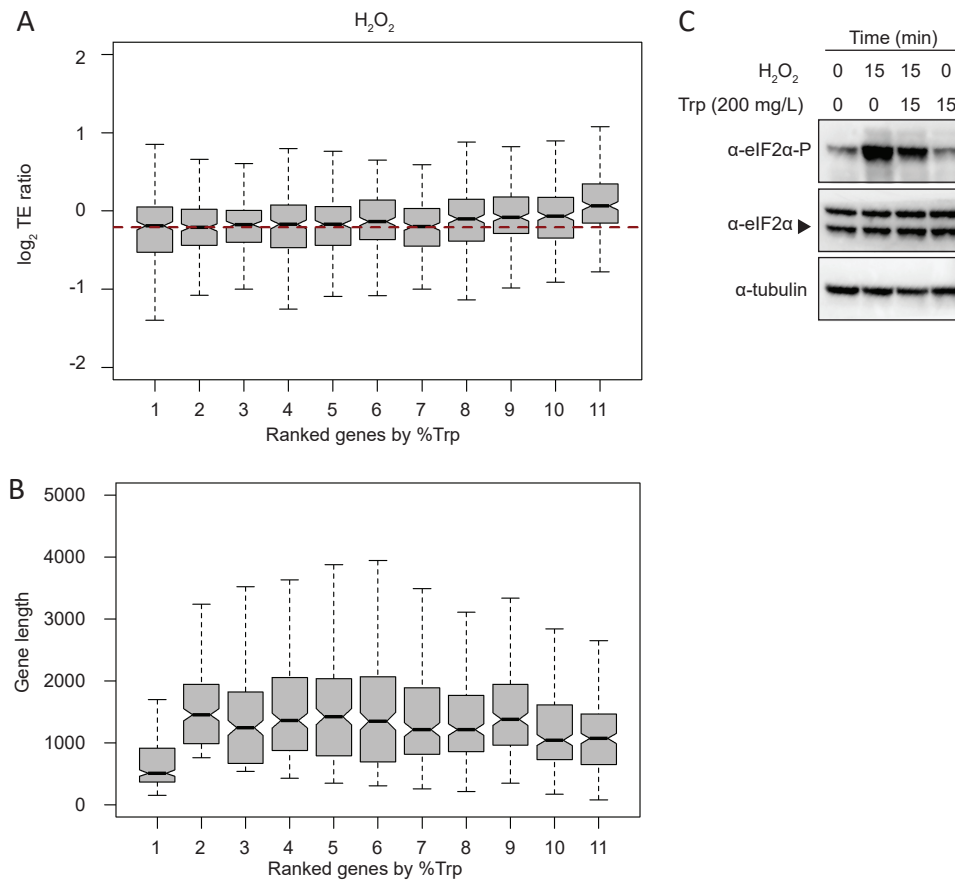


**Fig. 4. Role of Fil1 in the transcriptional responses to stress. (A to C)** Boxplots comparing mRNA levels of stressed and control cells ( $\log_2$  ratios stress/control) of Fil1 targets. Data are shown for wild type and *fil1Δ* cells at the indicated times and stresses **(D)** Venn diagram showing the overlap between genes expressed at low levels in *fil1Δ* mutant relative to wild type cells after heat shock (15 min), and Fil1 targets in unstressed cells. The P value of the observed overlap is shown. **(E)** As in D, but genes expressed at low levels in *fil1Δ* mutant relative to wild type after H<sub>2</sub>O<sub>2</sub> treatment (60 min) were compared to Fil1 targets in unstressed cells. **(F)** Drop assays of wild type and *fil1Δ* cells plated in the indicated conditions.

Figure 5

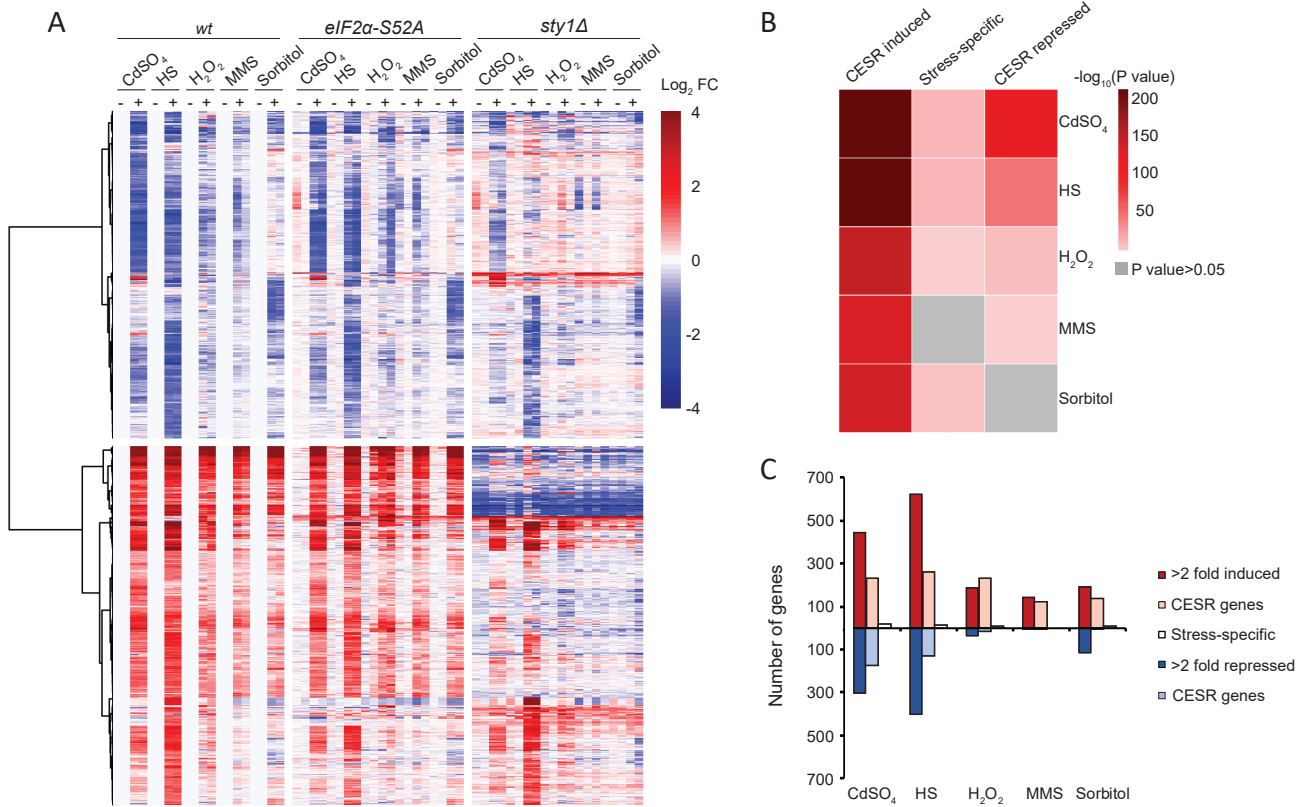


**Fig. 5. Levels of charged tRNA-Trp are affected by oxidative stress.** **(A)** Scatter plots showing  $\log_2$  relative codon enrichments before and after  $\text{H}_2\text{O}_2$  treatment for 15 minutes in wild type cells. The TGG codon encoding tryptophan is plotted in black. **(B)** Representative northern blot for the determination of tRNA-Trp charging levels before and after  $\text{H}_2\text{O}_2$  exposure. The top blot was hybridised with a probe against tRNA-Trp, and the bottom one with a probe against the U5 snRNA. In the upper blot, the top band corresponds to charged tRNA, and the bottom to the uncharged form. tRNA-Trp samples were either deacylated to remove the linked amino acid from charged tRNAs (sample D) or oxidised to remove the unprotected 3' nucleotides from uncharged tRNAs by beta-elimination (sample B-e) (see Methods for details). U5 snRNA was used as a loading control. **(C)** Quantification of tRNA-Trp charging ratios. Ratios between charged and uncharged tRNA were calculated, and normalised to the ratio in untreated cells. Each dot corresponds to an independent biological replicate ( $n = 5$ ), and the horizontal line indicates the mean. Significance was calculated by using a paired Student's t test. **(D)** As in C, but using a probe against tRNA-His (top panel) or U5 snRNA (bottom). **(E)** Northern blot as in C, to explore the effects of supplementing the culture medium with tryptophan. Cells were grown in the presence of tryptophan for 0, 15 or 120 min, and  $\text{H}_2\text{O}_2$  was added at the indicated times (0, 15 min) before the end of the incubation with tryptophan. Control deacylated RNA (sample D) is used to identify the location of uncharged tRNA. **(F)** Changes in intracellular tryptophan levels in response to  $\text{H}_2\text{O}_2$  exposure. Tryptophan levels were measured at the indicated times after  $\text{H}_2\text{O}_2$  addition to the culture medium. Each dot corresponds to an independent biological replicate ( $n = 4$ ), and the horizontal lines indicate the means. Significance was calculated using a paired Student's t test. No adjustment for multiple testing was performed.



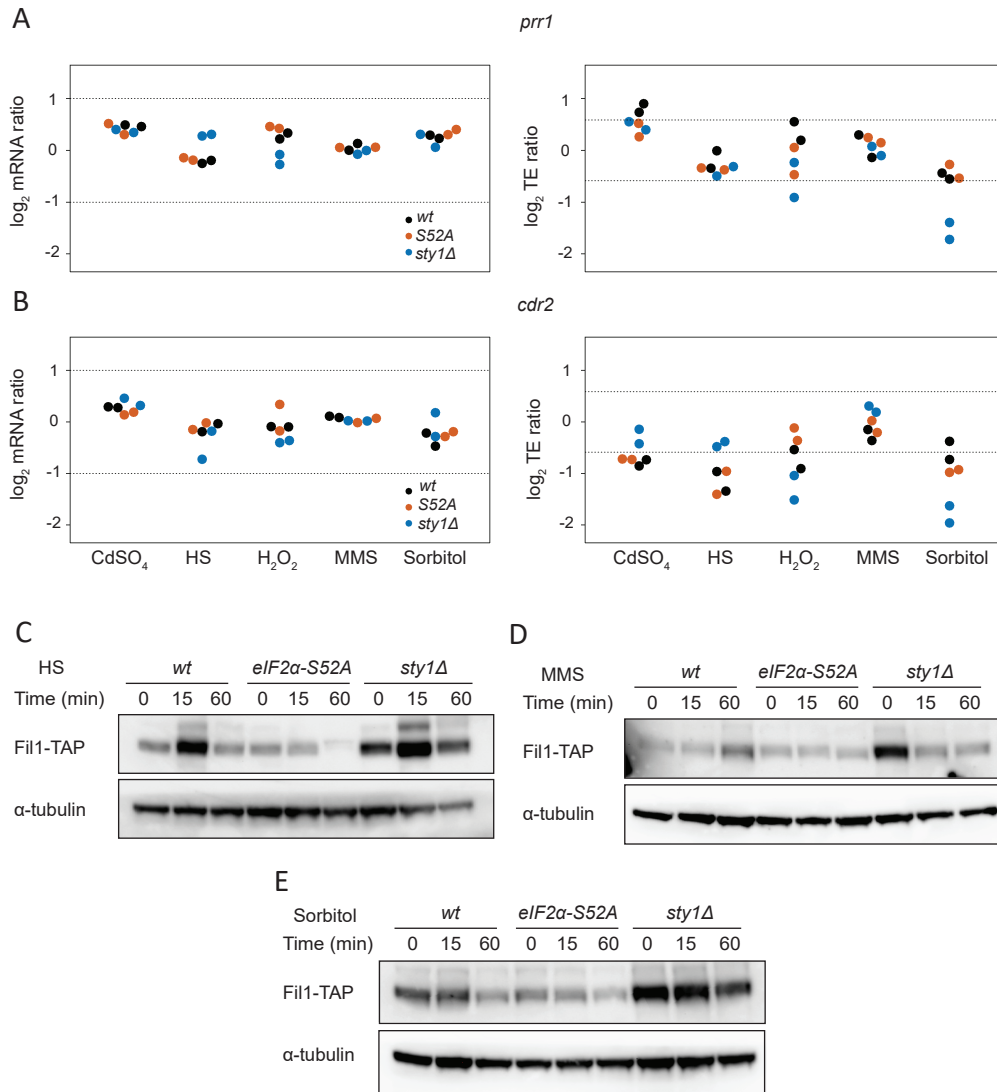
**Fig. 6. Oxidative stress affects the translation efficiency of tryptophan-enriched genes, and decreased tRNA-Trp charging may affect eIF2 $\alpha$  phosphorylation. (A)** Boxplots showing changes in translation efficiency upon oxidative stress ( $\log_2$  TE ratios stress/control, 15 min treatment) according to tryptophan content. Genes were binned into 11 categories based on the fraction of tryptophan in their coding sequences (the first group contains 269 genes without tryptophan, and the other 10 groups have 234 genes each). The horizontal red dashed line indicates the median of the second group. **(B)** As above, but displaying coding sequence lengths. **(C)** Western blots to investigate the effect of tryptophan on eIF2 $\alpha$  phosphorylation levels after  $H_2O_2$  treatment. Cells were treated with  $H_2O_2$  for 15 minutes and supplemental tryptophan was added as indicated. Tubulin was used as a loading control.





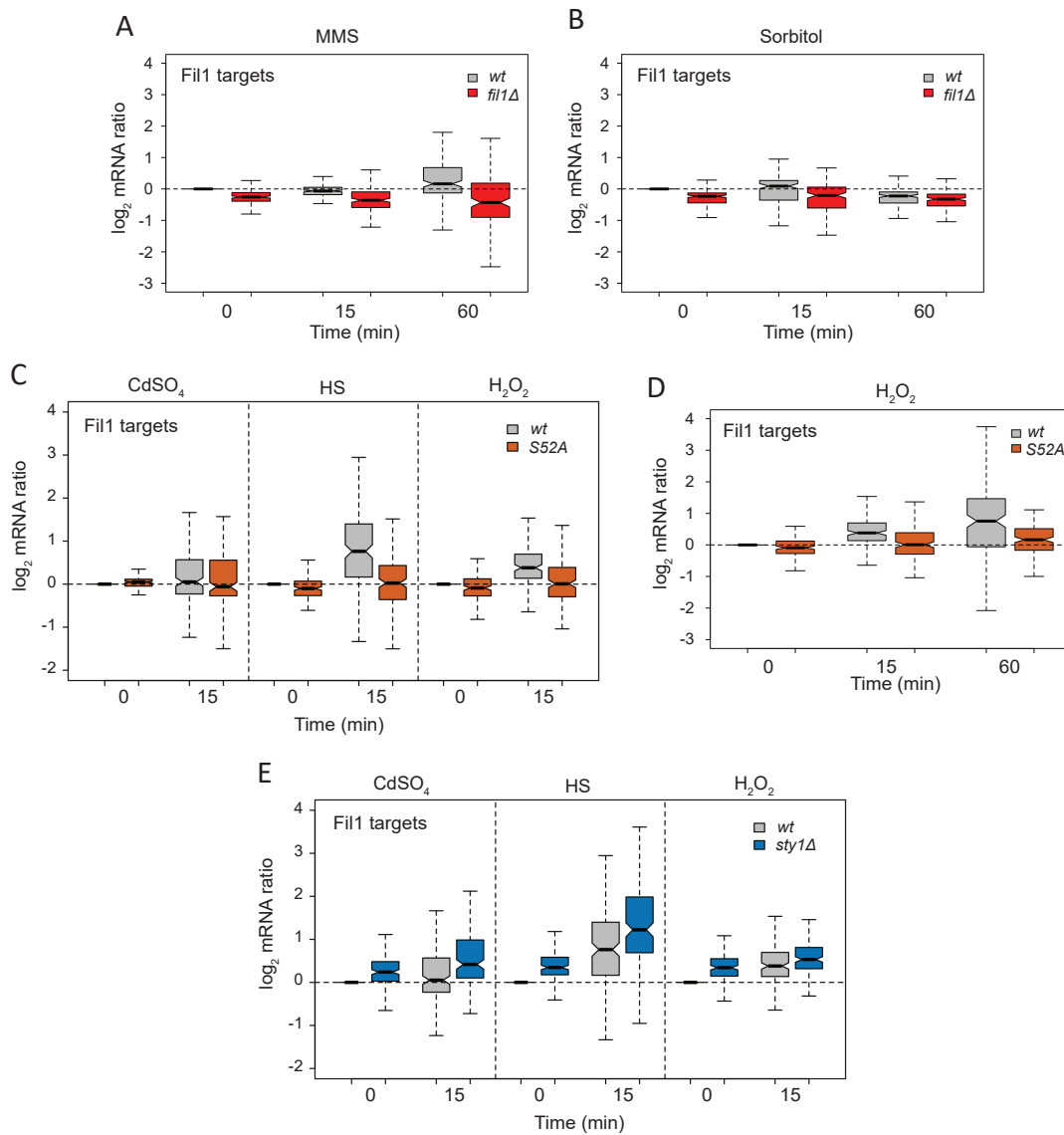
**Fig. S1. Transcriptomic responses to stress. (A)** Heat map of changes in mRNA levels in response to five stress conditions ( $\log_2$  ratio stress/control). Data are shown for 1,247 genes that are differentially expressed in at least one stress in wild type (see Methods for details). All data are normalised to the corresponding untreated wild type sample. **(B)** Heat map displaying enrichment analysis of previously described CCSR gene lists [14] and genes differentially expressed during five stress treatments (our dataset). **(C)** Comparison of the absolute numbers of induced and repressed genes in our experiments (>2-fold repressed or induced) with the CCSR-induced, CCSR-repressed and stress-specific genes [14].

Figure S2



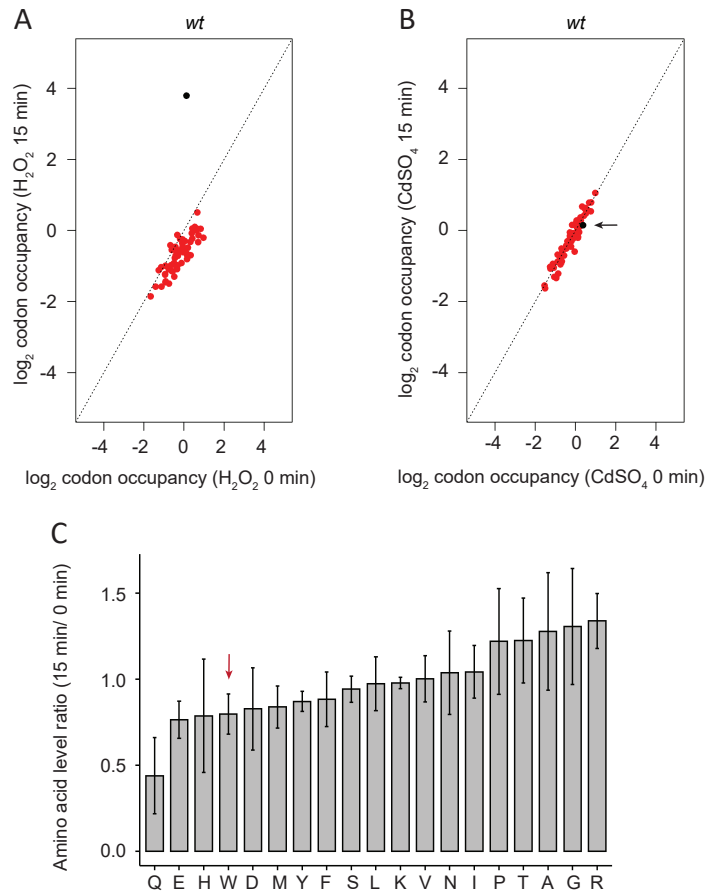
**Fig. S2. Gene-specific translational regulation.** (A) Changes in translation efficiency and transcript levels ( $\log_2$  ratios stress/control) obtained for the *prr1* gene. Data for two biological replicates are shown. (B) As in A, but for the *cdr2* gene. (C to E) Western blots to measure Fil1-TAP protein levels after heat shock, MMS and sorbitol at the indicated times and genetic backgrounds. Tubulin was used as a loading control.

Figure S3



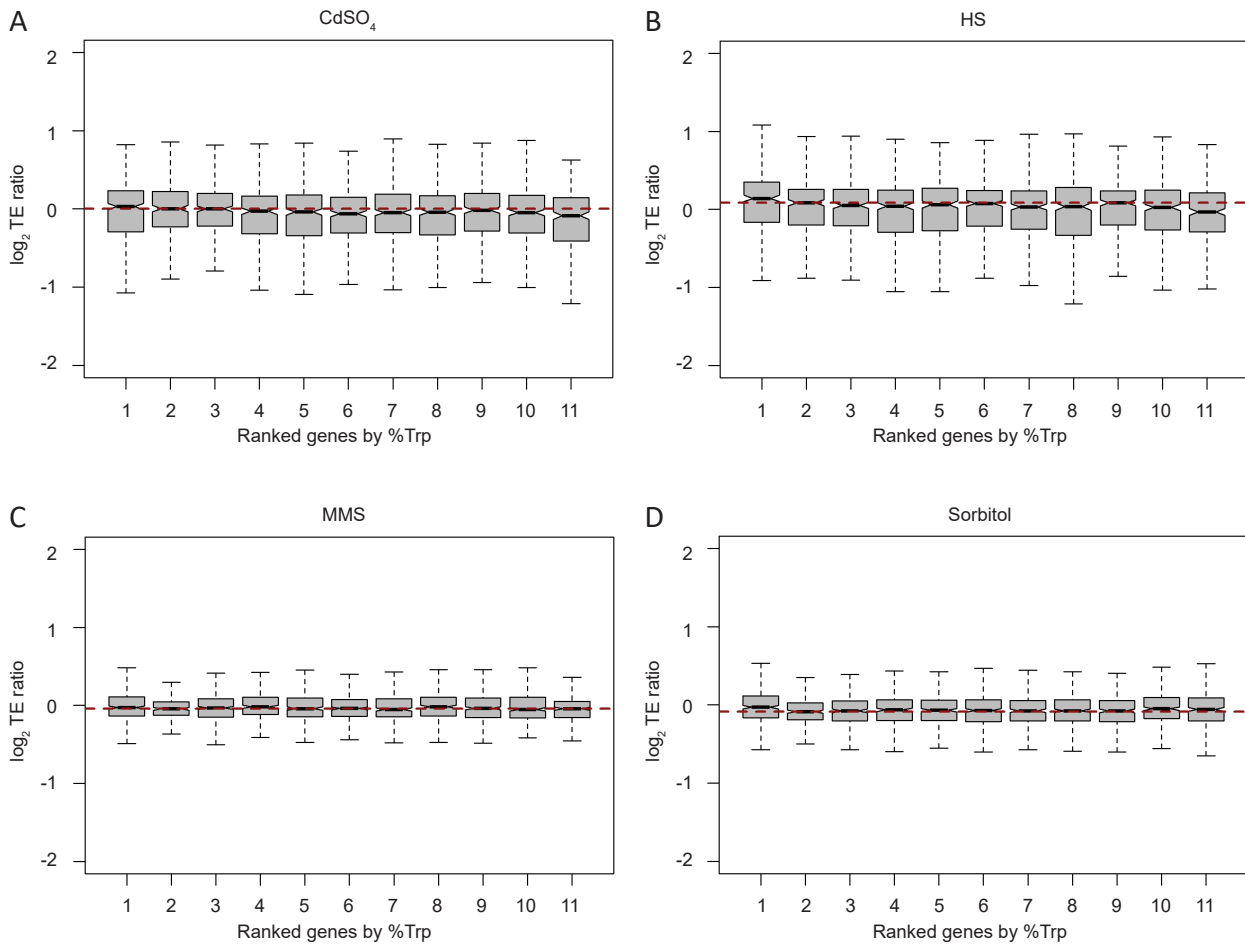
**Fig. S3. Transcription of Fil1 targets relies on eIF2 $\alpha$  phosphorylation and is increased in unstressed *sty1Δ* cells. (A and B)** Boxplot showing changes in mRNA levels ( $\log_2$  ratio stress/control) of genes encoding Fil1 targets after MMS and sorbitol treatments, in wild type and *fil1Δ* strains. **(C)** As in A and B, but after cadmium, heat shock and H<sub>2</sub>O<sub>2</sub> treatments, in wild type and *eIF2 $\alpha$ -S52A* strains. **(D)** As in C, but after H<sub>2</sub>O<sub>2</sub> treatment and with an additional time point. **(E)** As in C, but in the wild type and *sty1Δ* strains.

Figure S4



**Fig. S4. Tryptophan codon enrichment is specific for  $H_2O_2$  treatment.** (A) Scatter plots showing  $\log_2$  relative codon enrichments before and after  $H_2O_2$  treatment for 15 minutes in wild type cells (similar to Fig. 5A, but a different biological replicate). The TGG codon encoding tryptophan is plotted in black. (B) As in A, after cadmium treatment. TGG is displayed in black and highlighted with an arrow. (C) Change in amino acid levels (ratio stress/control) upon oxidative stress exposure. Data are from 4 independent biological replicates (means  $\pm$  SD). Tryptophan (W) is highlighted by a red arrow.

Figure S5



**Fig. S5. Translation efficiency of tryptophan-enriched genes after other stress treatments. (A to D)** Boxplots displaying changes in translation efficiency upon the indicated stresses ( $\log_2$  stress/control ratios) according to tryptophan content. Genes were binned into 11 categories based on the fraction of tryptophan in their coding sequences (the first group contains 269 genes lacking tryptophan, and the other 10 groups have 234 genes each). The horizontal red dashed line indicates the median of the second group.